

Breaking of k_{\perp} -factorization for Single Jet Production off Nuclei

N.N. Nikolaev^{a,b}, W. Schäfer^a)

^a*IKP(Theorie), Forschungszentrum Jülich, D-52425 Jülich, Germany*

^b*L.D. Landau Institute for Theoretical Physics, Moscow 117940, Russia*

E-mail: N.Nikolaev@fz-juelich.de; Wo.Schaefer@fz-juelich.de

Abstract

The linear k_{\perp} -factorization is part and parcel of the perturbative QCD description of high energy hard processes off free nucleons. In the case of heavy nuclear targets the very concept of nuclear parton density becomes ill-defined as exemplified by the recent derivation [2] of nonlinear nuclear k_{\perp} -factorization for forward dijet production in deep inelastic scattering off nuclei. Here we report a derivation of the related breaking of k_{\perp} -factorization for single-jet processes. We present a general formalism and apply it to several cases of practical interest: open charm and quark & gluon jet production in the central to beam fragmentation region of γ^*p, γ^*A, pp and pA collisions. We show how the pattern of k_{\perp} -factorization breaking and the nature and number of exchanged nuclear pomerons do change within the phase space of produced quark and gluon jets. As an application of the nonlinear k_{\perp} -factorization we discuss the Cronin effect. Our results are also applicable to the p_{\perp} -dependence of the Landau-Pomeranchuk-Migdal effect for, and nuclear quenching of, jets produced in the proton hemisphere of pA collisions.

PACS: 13.87.-a, 13.85.-t, 12.38.Bx, 11.80.La

I. INTRODUCTION

The familiar perturbative QCD (pQCD) factorization theorems tell that the hard scattering observables are linear functionals (convolutions) of the appropriate parton densities in the projectile and target [1] and are based on an implicit assumption that in the low-parton density limit the unitarity constraint can be ignored. They play, though, a fundamental role in interaction with strongly absorbing heavy nuclei which puts into question the very concept of a nuclear parton density. Indeed, a consistent analysis of forward hard dijet production in deep inelastic scattering (DIS) off nuclei revealed a striking breaking of k_{\perp} -factorization [2]: Namely, starting with the nuclear-shadowed nuclear DIS cross section, one can define the collective nuclear unintegrated gluon density such that the familiar linear k_{\perp} -factorization (see e.g. the recent reviews [3]) would hold for the forward single-quark spectrum but fail for the quark-antiquark two-jet spectrum which turns out to be a highly nonlinear functional of the collective nuclear gluon density. This finding casts a shadow on numerous extensions to nuclear collisions of the parton model formalism developed for nucleon-nucleon collisions and calls upon for revisiting other hard processes. The ultimate goal is the consistent description of nuclear effects from DIS to ultrarelativistic hadron-nucleus to (the initial stage of) nucleus-nucleus collisions, for instance at RHIC and LHC.

The purpose of this communication is a demonstration that the pattern of k_{\perp} -factorization breaking discovered in [2] holds also for a broad class of single-jet spectra. Here we recall that nuclear shadowing in DIS sets in at the Bjorken variable

$$x \lesssim x_A = \frac{1}{R_A m_N}, \quad (1)$$

when the coherency over the thickness of the nucleus holds for the $q\bar{q}$ Fock states of the virtual photon ([4, 5], for the color dipole phenomenology of the experimental data on nuclear shadowing see [6]). Here R_A is the radius of the target nucleus of mass number A and m_N is the proton mass. The analysis [2] focused on the excitation of quark and antiquark jets, $\gamma^* \rightarrow q\bar{q}$, in the photon fragmentation region at $x \lesssim x_A$. The subject of

this communication is excitation of open charm and jets,

$$g^* \rightarrow Q\bar{Q}, \quad g^* \rightarrow gg, \quad q^* \rightarrow qg, \quad (2)$$

in hadron–nucleon/nucleus scattering and/or DIS off nucleons and nuclei at $x \ll x_A$. At RHIC that means the large (pseudo)rapidity region of proton-proton and proton-nucleus collisions. Our starting point is the color dipole multiple scattering theory formulation of the open charm production in pA collisions [7] which we extend from the total to differential cross section and to arbitrary color state of the projectile parton. We treat the jet production at the pQCD parton level, our approach to the jet spectra is in many respects similar to Zakharov’s lightcone description of the QCD Landau-Pomeranchuk-Migdal (LPM) effect for the limit of thin targets [8, 9]. The results obtained below for the open charm and quark and gluon jets make manifest a change from linear to nonlinear k_{\perp} -factorization as the target changes from a free nucleon to heavy nucleus.

In the production of dijets in DIS [2] and πA collisions [10] the fragmenting particle was a color-singlet one. Here we consider the gN, gA, qN, qA collisions in which the beam partons are colored. In general the scattering of colored particles is plagued by infrared problems, but the excitation cross sections can be calculated as combinations of infrared-safe total cross sections for interaction with the target of certain color singlet multiparton states [2, 7, 8]. We discuss to some detail the so-called Cronin effect [11] - the nuclear antishadowing at moderate to large transverse momentum \mathbf{p} of jets. Decomposing in the spirit of the Leading $\text{Log}\mathbf{p}^2$ ($\text{LL}\mathbf{p}^2$) approximation the single-jet cross section into the so-called direct and resolved interactions of the incident parton we demonstrate that the Cronin effect is a salient feature of the resolved interactions and identify its origin to be the antishadowing nuclear higher-twist component of the collective gluon density of a nucleus derived in [12, 13]. Regarding the potential applications to pA collisions at RHIC we note that the k_{\perp} -factorization phenomenology of DIS [14] suggests fairly moderate $Q_A \sim 1$ GeV at $x \sim 10^{-2}$ for the heaviest nuclei [2], but we find that interesting nuclear effects extend to the pQCD domain of jet transverse momenta way beyond Q_A . Qualitatively similar results would be expected in a regime of strong

absorptive corrections also for hadronic targets other than nuclei, the nucleus represents a theoretical laboratory, in which saturation effects are endowed with a large parameter, the nuclear opacity, which allows for their systematic account.

One more point needs an emphasis. The partonic cross sections evaluated within the often used collinear approximation are subject to large smearing corrections for the so-called intrinsic transverse momentum $\langle p_T \rangle$ of partons, see [15]. In contrast to that we treat the pQCD partonic subprocesses with full allowance for the transverse momenta of all interacting partons and no extraneous $\langle p_T \rangle$ -smearing is needed. The discussion of nonperturbative effects such as nuclear modifications of the hadronization of jets ([16] and references therein) or of the recombination of partons into high- p_\perp hadrons ([17] and references therein) goes beyond the scope of the present study.

All our results are for the distribution of jets in both the transverse and longitudinal momentum, the latter is parameterized in terms of the fraction, z , of the longitudinal momentum of the incident parton a carried by the observed parton b . As such, they solve the LPM problem for finite transverse momentum \mathbf{p} , while the early works on the LPM effect focused on the \mathbf{p} -integrated longitudinal momentum spectrum. The \mathbf{p} -dependent LPM effect is important for a quantitative pQCD treatment of the nuclear quenching of forward high- \mathbf{p} hadrons observed experimentally by the BRAHMS collaboration [18]. The numerical results for the LPM effect for forward jets will be reported elsewhere, here we focus on the derivation and implications of the nonlinear k_\perp -factorization for the transverse momentum distributions.

The presentation of the main material is organized as follows. Our starting point is the color-dipole S -matrix representation for the two-body spectrum from the fragmentation $a \rightarrow bc$. We demonstrate how the single-parton cross spectrum can be calculated in terms of the S -matrices for special 2- and 3-body color singlet parton states (some technical details are given in Appendix A). The color-dipole master formulas for the single-parton spectra in interactions with free-nucleon and heavy-nucleus targets are reported in section III. They form the basis of the k_\perp -factorization representation for the spectra of different partons and in section IV we start with the linear, and in section V

with nonlinear, k_{\perp} -factorization for open charm production off free nucleons and nuclei, respectively. The subject of section VI is the Cronin effect in open charm production off nuclei. We demonstrate that in the general case the nuclear spectrum is a quadratic functional of the collective nuclear gluon density and illustrate this property in terms of the Kancheli-Mueller diagrams for inclusive cross sections [19]. The Cronin effect is shown to be a generic feature of the so-called resolved gluon interactions and its origin is attributed to the nuclear antishadowing property of the collective nuclear gluon density derived in [12]. We show that despite the relatively small saturation scale Q_A the Cronin effect extends to perturbatively large transverse momenta. In section VII we apply our master formula to the transverse momentum spectrum of gluons from the fragmentation $g^* \rightarrow gg$. In this case the nuclear cross section is a cubic functional of the collective nuclear gluon density. The subject of section VIII is the production of quark and gluon jets in the fragmentation $q^* \rightarrow qg$. The relevance of our results to the \mathbf{p} -dependent LPM effect is pointed out in sections VII and VIII. The main results are summarized and discussed in section IX. Our principal conclusion is that the k_{\perp} -factorization breaking is a universal feature of the pQCD description of hard processes in a nuclear environment. We comment on earlier works on single quark and gluon jet production [20–34], some of which invoke the Color Glass Condensate approach ([35] and references therein). A convenient technique of derivation of the n -parton interaction S-matrices is presented in Appendix A. The rules for the derivation of the wavefunctions of two-parton states in terms of the familiar splitting functions are given in Appendix B.

II. INCLUSIVE PRODUCTION AS EXCITATION OF FOCK STATES OF THE BEAM PARTON

Previously, the breaking of linear k_{\perp} -factorization had been demonstrated for the excitation of dijets, $\gamma^* \rightarrow q\bar{q}$, in DIS at $x \lesssim x_A$ [2]. Specifically, the two-parton transverse momentum spectrum was shown to be a highly nonlinear functional of the collective nuclear gluon density. On the other hand, upon integration over the transverse mo-

menta of the antiquark jet, the single-quark spectrum was found to fulfill the linear k_{\perp} -factorization. In this paper we extend the analysis of [2] to the case of colored beam partons, and confirm the breaking of k_{\perp} -factorization as a generic feature of the pQCD description of hard processes in a nuclear environment.

To the lowest order in pQCD the underlying subprocess for the mid- to large-rapidity open charm production in proton-proton collisions is the fusion of gluons from the beam and target, $gg \rightarrow c\bar{c}$; for the gluon jet production one would consider a collision of a beam quark with a gluon from the target, $qg \rightarrow qg$; at higher energies the relevant subprocess for gluon production will be $gg \rightarrow gg$. All the above processes are of the general form $ag \rightarrow bc$ and, from the laboratory frame standpoint, can be viewed as an excitation of the perturbative $|bc\rangle$ Fock state of the physical projectile $|a\rangle$ by one-gluon exchange with the target nucleon. In the case of a nuclear target one has to deal with multiple gluon exchanges which are enhanced by a large thickness of the target nucleus. A general treatment of multiple gluon exchanges in nuclear targets has been developed in [2, 7], its extension to the $a \rightarrow bc$ transitions can be described as follows:

Partons with energy E_a and transverse momentum \mathbf{p}_a such that

$$\frac{2m_N E_a}{\mathbf{p}_a^2} \gtrsim \frac{1}{x_A} \quad (3)$$

propagate along straight-line, fixed-impact-parameter, trajectories and interact coherently with the nucleus, which is behind the powerful color dipole formalism [5, 36, 37]. The target frame rapidity structure of the considered $a \rightarrow bc$ excitation is shown in fig. 1. The beam parton has a rapidity $\eta_a > \eta_A = \log 1/x_A$, the final state partons too have rapidities $\eta_{b,c} > \eta_A$. In this paper we focus on the lowest order excitation processes $a \rightarrow bc$ without production of more secondary partons in the rapidity span between η_b and η_c .

To the lowest order in the perturbative transition $a \rightarrow bc$ the Fock state expansion for the physical state $|a\rangle_{phys}$ reads

$$|a\rangle_{phys} = |a\rangle_0 + \Psi(z_b, \mathbf{r})|bc\rangle_0 \quad (4)$$

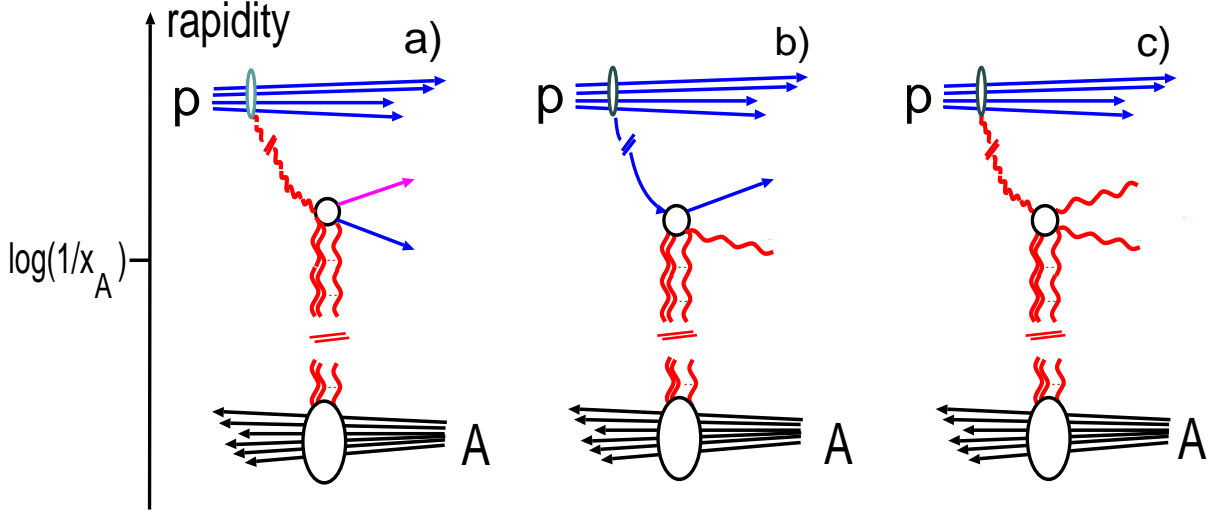


FIG. 1: (Color online) The rapidity structure of the excitation $a \rightarrow bc$: (a) excitation of mid- to large-rapidity open charm $g \rightarrow Q\bar{Q}$, (b) radiation of gluons by quarks $q \rightarrow qq$, (c) radiation of gluons by gluons $g \rightarrow gg$.

where $\Psi(z_b, \mathbf{r})$ is the probability amplitude to find the bc system with the separation \mathbf{r} in the two-dimensional impact parameter space, the subscript "0" refers to bare partons. The perturbative coupling of the $a \rightarrow bc$ transition is reabsorbed into the lightcone wave function $\Psi(z_b, \mathbf{r})$, and we also omitted a wave function renormalization factor, which is of no relevance for the inelastic excitation to the perturbative order discussed here.

If $\mathbf{b}_a = \mathbf{b}$ is the impact parameter of the projectile a , then

$$\mathbf{b}_b = \mathbf{b} + z_c \mathbf{r}, \quad \mathbf{b}_c = \mathbf{b} - z_b \mathbf{r}, \quad (5)$$

see Fig. 2. Here $z_{b,c}$ stand for the fraction the lightcone momentum of the projectile a carried by the partons b and c . The virtuality of the incident parton a is given by $Q_a^2 = \mathbf{k}_a^2$, where \mathbf{k}_a is the transverse momentum of the parton a in the incident proton (Fig. 1). For the sake of simplicity we take the collision axis along the momentum of parton a . The transformation between the transverse momenta in the a -target and p -target reference frames is trivial, $\mathbf{p}_{b,c}^{(a)} = \mathbf{p}_{b,c}^{(p)} + z_{c,b} \mathbf{k}_a$, below we cite all the spectra in the a -target collision frame. We shall speak of the produced parton - or jet originating from

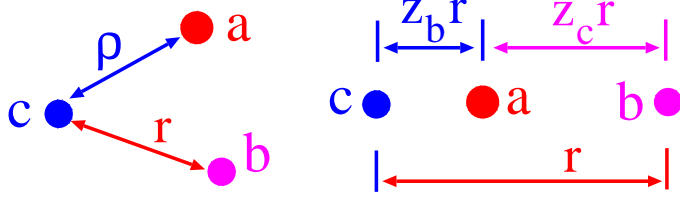


FIG. 2: (Color online) The color dipole structure (lhs) of the generic 3-parton state and (rhs) of the 3-parton state entering the color-dipole description of fragmentation $a \rightarrow bc$ with formation of the bc dipole of size \mathbf{r} .

this parton - as the *leading* one if it carries a fraction of the beam lightcone momentum $z \rightarrow 1$ and a *slow* one if it is produced with $z \ll 1$. We speak of the produced parton as a *hard* one if it is produced with large transverse momentum and a *soft* one if its transverse momentum is small compared to the so-called nuclear saturation scale to be defined below.

By the conservation of impact parameters, the action of the S -matrix on $|a\rangle_{phys}$ takes a simple form

$$\begin{aligned} S|a\rangle_{phys} &= S_a(\mathbf{b})|a\rangle_0 + S_b(\mathbf{b}_b)S_c(\mathbf{b}_c)\Psi(z_b, \mathbf{r})|bc\rangle_0 \\ &= S_a(\mathbf{b})|a\rangle_{phys} + [S_b(\mathbf{b}_b)S_c(\mathbf{b}_c) - S_a(\mathbf{b})]\Psi(z_b, \mathbf{r})|bc\rangle. \end{aligned} \quad (6)$$

In the last line we explicitly decomposed the final state into the elastically scattered $|a\rangle_{phys}$ and the excited state $|bc\rangle$. The two terms in the latter describe a scattering on the target of the bc system formed way in front of the target and the transition $a \rightarrow bc$ after the interaction of the state $|a\rangle_0$ with the target, as illustrated in fig. 3. The contribution from transitions $a \rightarrow bc$ inside the target nucleus vanishes in the high-energy limit

$$x = \frac{Q_a^2 + M_{bc}^2}{W^2 x_B} \lesssim x_A \quad (7)$$

where M_{bc} is the invariant mass of the excited bc system, Q_a^2 is the virtuality of the incident parton a , W is the total energy in the beam-target nucleon collision center of mass frame and x_B is the fraction of the beam energy carried by the beam-parton a .

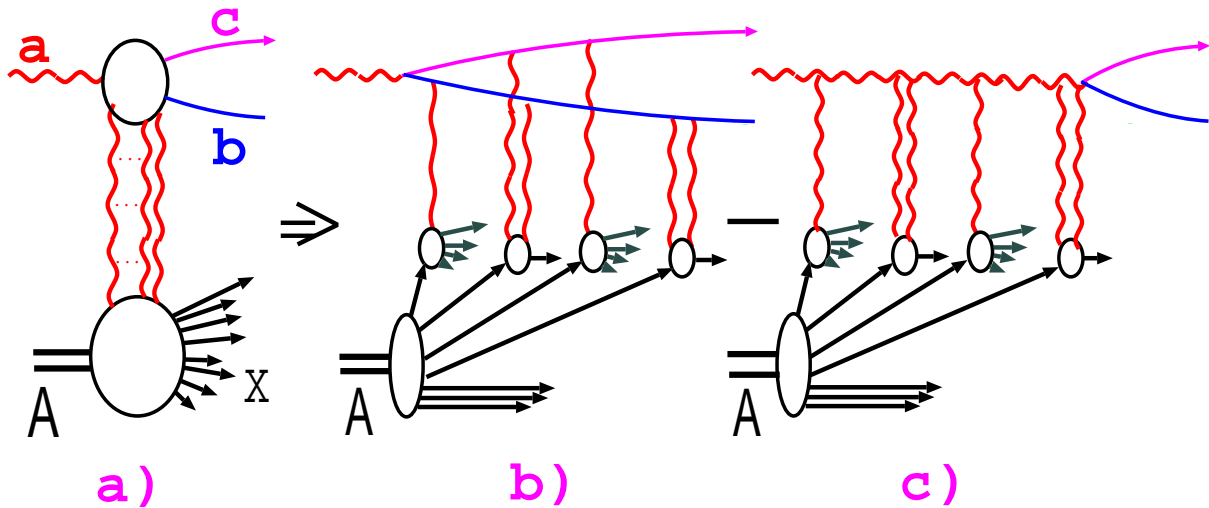


FIG. 3: (Color online) Typical contribution to the excitation amplitude for $gA \rightarrow q\bar{q}X$, with multiple color excitations of the nucleus. The amplitude receives contributions from processes that involve interactions with the nucleus after and before the virtual decay which interfere destructively.

The probability amplitude for the two-jet spectrum is given by the Fourier transform

$$\int d^2\mathbf{b}_b d^2\mathbf{b}_c \exp[-i(\mathbf{p}_b \mathbf{b}_b + \mathbf{p}_c \mathbf{b}_c)] [S_b(\mathbf{b}_b) S_c(\mathbf{b}_c) - S_a(\mathbf{b})] \Psi(z_b, \mathbf{r}) \quad (8)$$

The differential cross section is proportional to the modulus squared of (8) and one encounters the contributions containing

$$\begin{aligned} S_{\bar{a}a}^{(2)}(\mathbf{b}', \mathbf{b}) &= S_a^\dagger(\mathbf{b}') S_a(\mathbf{b}) \\ S_{\bar{a}bc}^{(3)}(\mathbf{b}', \mathbf{b}_b, \mathbf{b}_c) &= S_a^\dagger(\mathbf{b}') S_b(\mathbf{b}_b) S_c(\mathbf{b}_c), \\ S_{\bar{b}\bar{c}a}^{(3)}(\mathbf{b}, \mathbf{b}'_b, \mathbf{b}'_c) &= S_b^\dagger(\mathbf{b}'_b) S_c^\dagger(\mathbf{b}'_c) S_a(\mathbf{b}) \\ S_{\bar{b}\bar{c}cb}^{(4)}(\mathbf{b}'_b, \mathbf{b}'_c, \mathbf{b}_b, \mathbf{b}_c) &= S_b^\dagger(\mathbf{b}'_b) S_c^\dagger(\mathbf{b}'_c) S_c(\mathbf{b}_c) S_b(\mathbf{b}_b). \end{aligned} \quad (9)$$

Here we suppressed the matrix elements of $S^{(n)}$ over the target nucleon, for details see [2]. In the calculation of the inclusive cross sections one averages over the color states of the beam parton a , sums over color states of final state partons b, c and takes the matrix

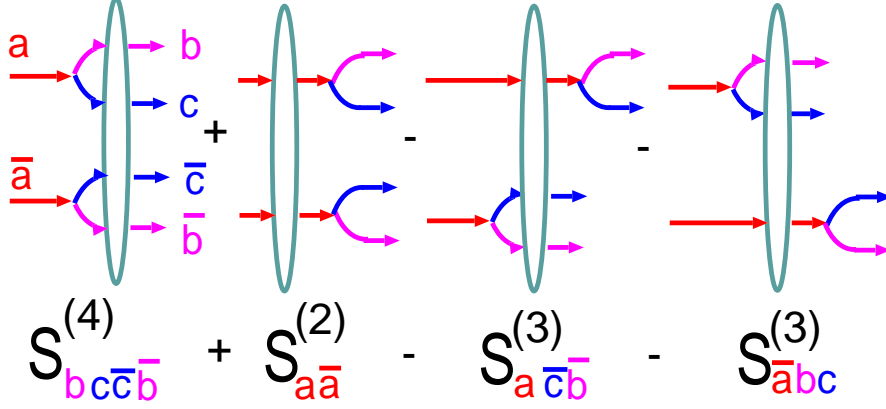


FIG. 4: (Color online) The S-matrix structure of the two-body density matrix for excitation $a \rightarrow bc$.

products of S^\dagger and S with respect to the relevant color indices entering $S^{(n)}$. Some of the technicalities of the derivation of $S^{(n)}$ are presented in the Appendix A, here we cite the resulting two-jet cross section:

$$\begin{aligned} \frac{d\sigma(a^* \rightarrow b(\mathbf{p}_b)c(\mathbf{p}_c))}{dzd^2\mathbf{p}_bd^2\mathbf{p}_c} &= \frac{1}{(2\pi)^4} \int d^2\mathbf{b}_bd^2\mathbf{b}_cd^2\mathbf{b}'_bd^2\mathbf{b}'_c \\ &\times \exp[i\mathbf{p}_b(\mathbf{b}_b - \mathbf{b}'_b) + i\mathbf{p}_c(\mathbf{b}_c - \mathbf{b}'_c)] \Psi(z, \mathbf{b}_b - \mathbf{b}_c) \Psi^*(z, \mathbf{b}'_b - \mathbf{b}'_c) \\ &\{S_{\bar{b}c\bar{c}\bar{b}}^{(4)}(\mathbf{b}'_b, \mathbf{b}'_c, \mathbf{b}_b, \mathbf{b}_c) + S_{a\bar{a}}^{(2)}(\mathbf{b}', \mathbf{b}) - S_{\bar{b}c\bar{a}}^{(3)}(\mathbf{b}, \mathbf{b}'_b, \mathbf{b}'_c) - S_{\bar{a}bc}^{(3)}(\mathbf{b}', \mathbf{b}_b, \mathbf{b}_c)\} \end{aligned} \quad (10)$$

The crucial point is that the hermitian conjugate S^\dagger can be viewed as the S -matrix for an antiparton [2, 7, 38]. As a result, $S_{a\bar{a}}^{(2)}(\mathbf{b}', \mathbf{b})$ is an S -matrix for interaction with the target of the $a\bar{a}$ state in which the antiparton \bar{a} propagates at the impact parameter \mathbf{b}' . The averaging over the color states of the beam parton a amounts to taking the color singlet $a\bar{a}$ state. The $S_{\bar{a}bc}^{(3)}$ and $S_{\bar{b}c\bar{c}\bar{b}}^{(4)}$ describe interaction of the color-singlet $\bar{a}bc$ and $\bar{b}c\bar{c}\bar{b}$ states, respectively. This is shown schematically in Fig. 4.

The $S^{(2)}$ and $S^{(3)}$ are readily calculated in terms of the 2-parton and 3-parton dipole cross sections [5, 7, 37], general rules for multiple scattering theory calculation of the coupled-channel $S^{(4)}$ are found in [2] and need not be repeated here.

The results for the two-jet cross sections will be presented elsewhere, here we focus on

the single-jet problem. Integration over the transverse momentum \mathbf{p}_c of the jet c gives

$$\mathbf{b}_c = \mathbf{b}'_c, \quad (11)$$

$$\mathbf{b} - \mathbf{b}' = z_b(\mathbf{r} - \mathbf{r}'), \quad \mathbf{b}_b - \mathbf{b}'_b = \mathbf{r} - \mathbf{r}', \quad \mathbf{b}' - \mathbf{b}_c = z_b \mathbf{r}'. \quad (12)$$

In the generic case the 3-parton state $\bar{a}bc$ has the dipole structure shown in Fig. 2 and the dipole cross section $\sigma_{3\bar{a}bc}(\boldsymbol{\rho}, \mathbf{r})$. In the considered problem of the $a \rightarrow bc$ excitation $\boldsymbol{\rho} = z_b \mathbf{r}'$. The case of $S_{\bar{b}cb}^{(4)}$ deserves special scrutiny. In the general case, $S^{(4)}$ is a multichannel operator, an example is found in [2]. Because in the single-particle spectrum $\mathbf{b}'_c = \mathbf{b}_c$, the unitarity relation

$$S_c^\dagger(\mathbf{b}_c) S_c(\mathbf{b}_c) = 1 \quad (13)$$

leads to a fundamental simplification of $S_{\bar{b}cb}^{(4)}(\mathbf{b}'_b, \mathbf{b}'_c, \mathbf{b}_b, \mathbf{b}_c)$. Specifically, in a somewhat symbolic form

$$S_{\bar{b}cb}^{(4)}(\mathbf{b}'_b, \mathbf{b}'_c, \mathbf{b}_b, \mathbf{b}_c) = S_b^\dagger(\mathbf{b}'_b) S_c^\dagger(\mathbf{b}_c) S_c(\mathbf{b}_c) S_b(\mathbf{b}_b) = S_b^\dagger(\mathbf{b}'_b) S_b(\mathbf{b}_b) = S_{\bar{b}b}^{(2)}(\mathbf{b}'_b, \mathbf{b}_b), \quad (14)$$

i.e., the effect of interactions of the spectator parton c vanishes upon the summation over all its color states and integration over all its transverse momenta [7]. The coupled-channel operator $S_{\bar{b}cb}^{(4)}$ then takes a single-channel form, some technical points behind this derivation are clarified in Appendix A. The only trace of the observed parton b having been produced in the fragmentation $a \rightarrow bc$ is in the density matrix $\Psi(z_b, \mathbf{b}_b - \mathbf{b}_c) \Psi^*(z_b, \mathbf{b}'_b - \mathbf{b}'_c)$ which defines the transverse momentum distribution of the parton b in the beam parton a and the partition $z_b, z_c = (1 - z_b)$, of the longitudinal momentum between the final state partons. It will be more convenient to regard $S_{\bar{b}b}^{(2)}(\mathbf{b}'_b, \mathbf{b}_b)$ as a function of the transverse size of the $b\bar{b}$ dipole $\mathbf{b}'_b - \mathbf{b}_b$, and the impact parameter \mathbf{B} of the dipole–nucleus interaction, and we shall from now on write $S_{\bar{b}b}^{(2)}(\mathbf{b}'_b, \mathbf{b}_b) \rightarrow S_{\bar{b}b}^{(2)}(\mathbf{B}, \mathbf{b}'_b - \mathbf{b}_b)$.

The observation (14) can be generalized further to the cancellations of beam spectator interactions. The detailed discussion will be reported elsewhere, here we just quote the simple example of open heavy flavour excitation. The above expounded formalism for the fragmentation $g \rightarrow Q\bar{Q}$ can readily be generalized to excitation of heavy flavour from

the incident quark $q^* \rightarrow q'Q\bar{Q}$ which proceeds via $q^* \rightarrow q'g$, $g \rightarrow Q\bar{Q}$. The simplest case of direct importance for mid-rapidity heavy flavour production in pp, pA collisions is when the produced $Q\bar{Q}$ pair carries a small fraction of the incident quark's momentum, i.e., the underlying partonic subprocess is a collision of a slow gluon from the beam with a slow gluon from the target, $gg \rightarrow Q\bar{Q}$. The generalization of eqs. (11), (12) to this case shows that the beam quark q^* and the spectator quark q' would propagate at the same impact parameter \mathbf{b}_q . One readily finds that the amplitude of the $q^* \rightarrow q'Q\bar{Q}$ will be given by eq. (6) times the extra factor of $S_q(\mathbf{b}_q)$. Upon the integration over the transverse momentum of the spectator quark one gets the equality of the corresponding impact parameters in the multiparton S -matrix and its hermitian conjugate, eq. (11), and upon the application of the unitarity relation (13) the effect of spectator interactions cancels out in complete analogy to eq. (14). The resulting $S_{\bar{b}b}^{(2)}(\mathbf{B}, \mathbf{b}'_b - \mathbf{b}_b)$ only depends on the dipole parameter $\mathbf{b}'_b - \mathbf{b}_b$ and the overall impact parameter, \mathbf{B} , of the multiparton system. What will be left of the beam quark q^* is the wave function of its $q'g$ Fock state which defines the longitudinal and transverse momentum density in the beam of the gluon g^* which excites into the $Q\bar{Q}$ state. The evident assumption behind the spectator interaction cancellations is that the coherency condition is fulfilled for all spectator partons; because the spectators are faster than the observed parton, this weak condition does not impose any stringent constraints beyond (7).

III. COLOR DIPOLE MASTER FORMULA FOR FREE NUCLEONS AND NUCLEI

For the free nucleon target integration over the impact parameter \mathbf{B} gives the corresponding total cross sections, for instance,

$$\begin{aligned}
2 \int d^2\mathbf{B} \left[1 - S_{\bar{b}b}^{(2)}(\mathbf{B}, \mathbf{b}'_b - \mathbf{b}_b) \right] &= \sigma_{2,\bar{b}b}(\mathbf{r} - \mathbf{r}') \\
2 \int d^2\mathbf{B} \left[1 - S_{\bar{a}bc}^{(3)}(\mathbf{B}, \mathbf{b}' - \mathbf{b}_c, \mathbf{b}_b - \mathbf{b}_c) \right] &= \sigma_{3,\bar{a}bc}(z_b\mathbf{r}', \mathbf{r}).
\end{aligned} \tag{15}$$

Then the single-jet spectrum for the free nucleon target can be cast in the form

$$\begin{aligned} \frac{d\sigma_N(a^* \rightarrow b(\mathbf{p}_b)c)}{dz_b d^2\mathbf{p}_b} &= \frac{1}{2(2\pi)^2} \int d^2\mathbf{r} d^2\mathbf{r}' \exp[i\mathbf{p}_b(\mathbf{r} - \mathbf{r}')] \Psi(z_b, \mathbf{r}) \Psi^*(z_b, \mathbf{r}') \\ &\times \{ \sigma_{3,\bar{a}bc}(z_b \mathbf{r}', \mathbf{r}) + \sigma_{3,\bar{a}\bar{b}\bar{c}}(z_b \mathbf{r}, \mathbf{r}') - \sigma_{2,\bar{b}\bar{b}}(\mathbf{r} - \mathbf{r}') - \sigma_{2,\bar{a}\bar{a}}(z_b(\mathbf{r} - \mathbf{r}')) \} \end{aligned} \quad (16)$$

In the generic $\bar{a}bc$ system there could be more than one scheme of coupling to a color singlet state, in which case $S_{\bar{a}bc}^{(3)}$ would be a coupled-channel operator, but that is not the case with gluons and quarks. The coupled-channel operator $S_{\bar{b}\bar{c}cb}^{(4)}$ also takes the single-channel form (14). As usual, we apply multiple scattering theory treating the nucleus as a dilute gas of color-singlet nucleons, and upon the summation over all the nuclear final states and application of the closure relation the nuclear matrix elements of $S^{(n)}$ take the familiar Glauber-Gribov form [39, 40]. The resulting nuclear single-jet spectrum per unit area in the impact-parameter plane equals

$$\begin{aligned} \frac{d\sigma_A(a^* \rightarrow b(\mathbf{p}_b)c)}{dz d^2\mathbf{p}_b d^2\mathbf{b}} &= \frac{1}{(2\pi)^2} \int d^2\mathbf{r} d^2\mathbf{r}' \exp[i\mathbf{p}_b(\mathbf{r} - \mathbf{r}')] \Psi(z_b, \mathbf{r}) \Psi^*(z_b, \mathbf{r}') \\ &\times \left\{ \Gamma_A[\mathbf{b}, \sigma_{3,\bar{a}bc}(z_b \mathbf{r}', \mathbf{r})] + \Gamma_A[\mathbf{b}, \sigma_{3,\bar{a}\bar{b}\bar{c}}(z_b \mathbf{r}, \mathbf{r}')] \right. \\ &\left. - \Gamma_A[\mathbf{b}, \sigma_{2,\bar{b}\bar{b}}(\mathbf{r} - \mathbf{r}')] - \Gamma_A[\mathbf{b}, \sigma_{2,\bar{a}\bar{a}}(z_b(\mathbf{r} - \mathbf{r}'))] \right\}. \end{aligned} \quad (17)$$

We can use the Glauber-Gribov multiple scattering theory result

$$\Gamma_A[\mathbf{b}, \sigma] = 1 - \exp\left[-\frac{1}{2}\sigma T(\mathbf{b})\right], \quad (18)$$

where $T(\mathbf{b}) = \int_{-\infty}^{\infty} dr_z n_A(\mathbf{b}, r_z)$ is the optical thickness of the nucleus, and the nuclear density $n_A(\mathbf{b}, r_z)$ is normalized according to $\int d^3\vec{r} n_A(\mathbf{b}, r_z) = \int d^2\mathbf{b} T(\mathbf{b}) = A$.

Within the color-dipole formalism the x -dependence of the DIS structure function is driven by the x -dependence of the color-dipole cross section $\sigma_{q\bar{q}}(x, \mathbf{r})$ which is governed by the color-dipole form of the Balitskii–Fadin–Kuraev–Lipatov (BFKL) equation [37, 41, 42]. For $x \gtrsim x_A$ DIS off a nucleus amounts to the sum of incoherent scatterings off bound nucleons. The onset of nuclear coherence effects at $x \lesssim x_A$ must be treated with the color-dipole cross section $\sigma_{q\bar{q}}(x_A, \mathbf{r})$ which has been BFKL-evolved down to $x = x_A$. We recall that for heavy nuclei well evolved shadowing sets in at $x_A \approx 10^{-2}$. The considered

lowest order excitation processes $a \rightarrow bc$ with rapidities $\eta_{b,c} \gtrsim \eta_A$ such that no more secondary partons are produced in the rapidity span between η_b and η_c or between $\eta_{b,c}$ and η_A must also be treated in terms of $\sigma_{q\bar{q}}(x_A, \mathbf{r})$. The values of $x_{b,c}$ attainable at RHIC are such that jet production in the proton hemisphere of pA collisions at RHIC is dominated by precisely these lowest-order processes. The allowance for higher-order processes would amount to the x -evolution of the k_\perp -factorization breaking and will be addressed to elsewhere.

IV. k_\perp -FACTORIZATION FOR OPEN CHARM PRODUCTION OFF FREE NUCLEONS

Here the underlying pQCD excitation is $g \rightarrow Q\bar{Q}$, i.e., $a = g, b = Q, c = \bar{Q}$. The process is symmetric under $Q \leftrightarrow \bar{Q}$ and for the sake of brevity we we put $z \equiv z_Q$ and $\mathbf{p} \equiv \mathbf{p}_Q$. The relevant 2-parton and 3-parton dipole cross sections equal [7, 37]

$$\begin{aligned}\sigma_3(x, z\mathbf{r}', \mathbf{r}) &= \frac{C_A}{2C_F} [\sigma_{q\bar{q}}(x, z\mathbf{r}' - \mathbf{r}) + \sigma_{q\bar{q}}(x, z\mathbf{r}') - \sigma_{q\bar{q}}(x, \mathbf{r})] + \sigma_{q\bar{q}}(x, \mathbf{r}), \\ \sigma_{gg}(x, z(\mathbf{r} - \mathbf{r}')) &= \frac{C_A}{C_F} \sigma_{q\bar{q}}(x, z(\mathbf{r} - \mathbf{r}')), \end{aligned} \quad (19)$$

where $C_A = N_c$, $C_F = \frac{N_c^2 - 1}{2N_c}$ are the familiar quadratic Casimirs, and [43]

$$\begin{aligned}\sigma_{q\bar{q}}(x, \mathbf{r}) &= \int d^2\boldsymbol{\kappa} f(x, \boldsymbol{\kappa}) [1 - \exp(i\boldsymbol{\kappa}\mathbf{r})], \\ f(x, \boldsymbol{\kappa}) &= \frac{4\pi\alpha_S(r)}{N_c} \cdot \frac{1}{\kappa^4} \cdot \mathcal{F}(x, \kappa^2). \end{aligned} \quad (20)$$

$\sigma_{q\bar{q}}(x, \mathbf{r})$ is the dipole cross section for the $q\bar{q}$ color dipole and

$$\mathcal{F}(x, \kappa^2) = \frac{\partial G(x, \kappa^2)}{\partial \log \kappa^2} \quad (21)$$

is the unintegrated gluon density in the target nucleon (our normalization of $f(x_A, \boldsymbol{\kappa})$ and of the related Weizsäcker-Williams gluon density $\phi(\mathbf{b}, x_A, \boldsymbol{\kappa}) \equiv \phi_{WW}(\mathbf{b}, x_A, \boldsymbol{\kappa})$, see below, are slightly different from the ones used in [2]). In the momentum space calculations the running coupling $\alpha_S(r)$ must be taken at an appropriate hard scale.

Applying the technique developed in [2], upon the relevant Fourier transformations one readily finds

$$\begin{aligned} \frac{2(2\pi)^2 d\sigma_N(g^* \rightarrow Q\bar{Q})}{dzd^2\mathbf{p}} &= \int d^2\boldsymbol{\kappa} f(x_A, \boldsymbol{\kappa}) \\ &\left\{ \frac{N_c^2}{N_c^2 - 1} \left(|\Psi(z, \mathbf{p}) - \Psi(z, \mathbf{p} + z\boldsymbol{\kappa})|^2 + |\Psi(z, \mathbf{p} + \boldsymbol{\kappa}) - \Psi(z, \mathbf{p} + z\boldsymbol{\kappa})|^2 \right) \right. \\ &\left. + \frac{1}{N_c^2 - 1} |\Psi(z, \mathbf{p}) - \Psi(z, \mathbf{p} + \boldsymbol{\kappa})|^2 \right\} \end{aligned} \quad (22)$$

$$\begin{aligned} &= \int d^2\boldsymbol{\kappa} f(x_A, \boldsymbol{\kappa}) \left(\frac{C_A}{2C_F} \left\{ |\Psi(z, \mathbf{p}) - \Psi(z, \mathbf{p} + z\boldsymbol{\kappa})|^2 + |\Psi(z, \mathbf{p} + \boldsymbol{\kappa}) - \Psi(z, \mathbf{p} + z\boldsymbol{\kappa})|^2 \right. \right. \\ &\left. \left. - |\Psi(z, \mathbf{p}) - \Psi(z, \mathbf{p} + \boldsymbol{\kappa})|^2 \right\} + |\Psi(z, \mathbf{p}) - \Psi(z, \mathbf{p} + \boldsymbol{\kappa})|^2 \right). \end{aligned} \quad (23)$$

Here we show explicitly that the target gluon density $f(x_A, \boldsymbol{\kappa})$ enters with the boundary condition argument x_A . The expression $|\Psi(z, \mathbf{p}) - \Psi(z, \mathbf{p} + z\boldsymbol{\kappa})|^2$ for the $Q\bar{Q}$ Fock state of the gluon is obtained from its counterpart for the transverse photon cited in [2] by the substitutions $Q^2 \rightarrow Q_a^2$ and $N_c\alpha_{em}e_Q^2 \rightarrow T_F\alpha_S$, see Appendix B.

Here we emphasize that Eqns. (22,23) account fully for the transverse momenta of all involved partons, no further smearing of the obtained spectra for the intrinsic transverse momentum of partons is needed, furthermore, it would be illegitimate. Early discussions of charm production in hadron–nucleon collisions in the framework of k_\perp -factorization can be found in [44], for reviews and a guide to recent literature we refer to [3]. The rather straightforward representation (22,23) of the heavy quark cross section in terms of light–cone wavefunctions for the transition $g^* \rightarrow Q\bar{Q}$ is new, as are the related expressions for quark/gluon production to be found below.

Some comments on this simple formula are in order. First, although we spoke of the charm production, as soon as the transverse momentum \mathbf{p} is perturbatively large eq. (23) will fully be applicable to light quark jets and there is an obvious connection between (23) and the NLL real correction to the BFKL kernel from light $q\bar{q}$ pair production, but dwelling into that is beyond the scope of the present communication. Second, we presented our result for two different groupings of terms. While in the first grouping (22) the result is given as a manifestly positive sum of squares, in the second one (23) we

decomposed the cross section into 'nonabelian', $\propto C_A/2C_F$, and 'abelian' pieces. Putting $C_A \rightarrow 0$ one would switch off the nonabelian coupling of gluons to gluons and obtain indeed the same formula as for the single-quark spectrum from the $\gamma^* \rightarrow q\bar{q}$ transition, i.e., for inclusive DIS [2]. Third, note that the same 'abelian' limit is obtained at the boundaries $z = 0$ and $1 - z = 0$. In the both cases that can be traced to the fact either the spectator quark for $z = 0$, or the observed antiquark for $z = 1$ would propagate at precisely the same impact parameter as the parent gluon so that the non-abelian color structure of the $gQ\bar{Q}$ is simply not resolved. Still the physics of the two cases is different: in the limit of $z = 0$ the 'initial state' gg dipole interaction effectively drops out, whereas at $z = 1$ there are subtle cancellations between the gg dipole cross section and the octet-octet dipole components of the 3-parton cross sections. As we shall see below, the latter cancellations will be upset for nuclear targets. Fourth, in the large- N_c limit $C_A = 2C_F$ and for later reference we quote

$$\begin{aligned} & \frac{2(2\pi)^2 d\sigma_N(g^* \rightarrow Q\bar{Q})}{dzd^2\mathbf{p}} \Big|_{N_c \gg 1} = \\ & = \int d^2\boldsymbol{\kappa} f(x_A, \boldsymbol{\kappa}) \left\{ |\Psi(z, \mathbf{p}) - \Psi(z, \mathbf{p} + z\boldsymbol{\kappa})|^2 + |\Psi(z, \mathbf{p} + \boldsymbol{\kappa}) - \Psi(z, \mathbf{p} + z\boldsymbol{\kappa})|^2 \right\} \end{aligned} \quad (24)$$

Based on the discussion of spectator effects in section III and anticipating the discussion in section VI, we note that the open-charm production can be presented in a manifestly beam-target symmetric form. One can multiply the above derived cross section $d\sigma_Q^{(g^* \rightarrow Q\bar{Q})}(z, x_A, \mathbf{p})$ by the unintegrated flux of gluons of transverse momentum \mathbf{k}_a and lightcone momentum fraction x_B in the beam proton, $\mathcal{F}(x_B, \mathbf{k}_a)$, take the wave functions of Appendix B at $Q^2 = \mathbf{k}_a^2$, and calculate the charm spectrum for pp, pA collisions as

$$d\sigma_{N,A}(z, x_A, \mathbf{p}) = \frac{1}{x_B} \int d^2\mathbf{k}_a \mathcal{F}(x_B, \mathbf{k}_a) d\sigma_{N,A}^{(g^* \rightarrow Q\bar{Q})}(z, x_A, \mathbf{p} + z\mathbf{k}_a). \quad (25)$$

The usual kinematical constraint, $x_B x_A W^2 = \frac{\mathbf{p}^2 + m_Q^2}{z(1-z)}$, is understood. The fully inclusive single-parton cross section is obtained from (25) upon integration over x_B keeping fixed the longitudinal momentum of the observed parton zx_B . We stick to z because (i) the transverse momentum spectra exhibit a highly nontrivial dependence on z and (ii)

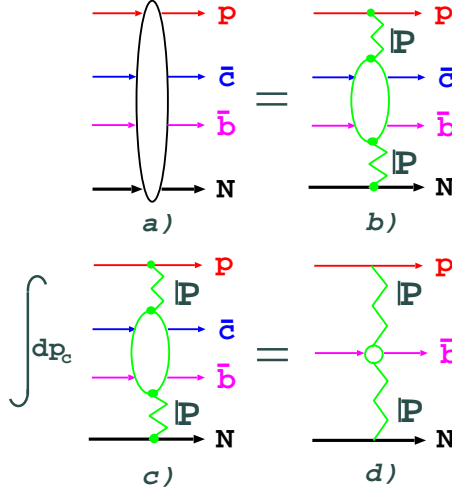


FIG. 5: (Color online) (a) The Kancheli-Mueller diagram for the two-parton inclusive cross section in proton-proton collisions, (b) its representation in terms of the pomeron exchange and (c) transition to the optical theorem for the single-parton inclusive cross section (d) upon the integration over the phase space of the parton c .

understanding the z -dependence is crucial for the LPM effect.

Within the k_{\perp} -factorization the microscopic QCD description of the pomeron exchange is furnished by the unintegrated gluon densities. To this end one can look at the open-charm cross section (25) through the prism of the Kancheli-Mueller diagrams [19] for inclusive spectra as depicted in a somewhat symbolic way in figure (5). The $\bar{c}b\mathbf{IP}\bar{c}b\mathbf{IP}$ vertex which enters the pomeron-exchange representation (b) for the generic Kancheli-Mueller discontinuity of the 4-body forward scattering amplitude is a highly nonlocal one, its properties will be discussed to more detail elsewhere. Upon integration over the momentum of the parton c one obtains the Kancheli-Mueller diagram (d) for the single-parton spectrum, for the nonlocal properties of the $\bar{b}\mathbf{IP}\bar{b}\mathbf{IP}$ vertex in the diagram (d) see Sect.VI D 1.

V. NUCLEAR CASE: NONLINEAR k_{\perp} -FACTORIZATION

The driving term of small- x nuclear structure functions and single-quark spectra from the $\gamma^* \rightarrow q\bar{q}$ excitation off a nucleus were shown to take the familiar k_{\perp} -factorization form in terms of the collective nuclear Weizsäcker–Williams gluon density $\phi(\mathbf{b}, x_A, \boldsymbol{\kappa})$ per unit area in the impact parameter plane as defined in [2, 12, 13, 45]:

$$\Gamma_A[\mathbf{b}, \sigma_{q\bar{q}}(x, \mathbf{r})] \equiv \int d^2\boldsymbol{\kappa} \phi(\mathbf{b}, x, \boldsymbol{\kappa}) [1 - \exp[i\boldsymbol{\kappa}\mathbf{r}]]. \quad (26)$$

It satisfies the sum rule

$$\int d^2\boldsymbol{\kappa} \phi(\mathbf{b}, x, \boldsymbol{\kappa}) = 1 - \exp[-\frac{1}{2}\sigma_0(x)T(\mathbf{b})] = 1 - S_{abs}(\mathbf{b}). \quad (27)$$

where $\sigma_0(x) = \int d^2\boldsymbol{\kappa} f(x, \boldsymbol{\kappa})$ is the dipole cross section for large dipoles. It is conveniently interpreted in the spirit of additive quark counting for soft hadronic processes as $\sigma_0(x) = \sigma_{qN}(x) + \sigma_{\bar{q}N}(x) = 2\sigma_{qN}^{\mathbf{P}}(x)$, so that the meaning of the factor

$$S_{abs}(\mathbf{b}) = \exp[-\frac{1}{2}\sigma_0(x)T(\mathbf{b})] = \exp[-\sigma_{qN}^{\mathbf{P}}(x)T(\mathbf{b})] \quad (28)$$

as representing intranuclear absorption becomes evident.

Eqs. (17), (19) and (20) allow a straightforward calculation of the nuclear single-jet spectra. Nice analytic forms of the nuclear k_{\perp} -factorization are obtained in the large- N_c limit, the $1/N_c^2$ corrections can readily be derived following the considerations in [2] and will not be discussed here. The crucial point about the large- N_c approximation is that

$$\begin{aligned} \sigma_3(x, z\mathbf{r}', \mathbf{r}) &\implies \sigma_{q\bar{q}}(x, z\mathbf{r}' - \mathbf{r}) + \sigma_{q\bar{q}}(x, z\mathbf{r}'), \\ \sigma_{gg}(x, z(\mathbf{r} - \mathbf{r}')) &\implies 2\sigma_{q\bar{q}}(x, z(\mathbf{r} - \mathbf{r}')) \end{aligned} \quad (29)$$

so that

$$\begin{aligned} \Gamma_A[\mathbf{b}, \sigma_3(z\mathbf{r}', \mathbf{r})] &= \Gamma_A[\mathbf{b}, \sigma_{q\bar{q}}(x, z\mathbf{r}' - \mathbf{r})] + \Gamma_A[\mathbf{b}, \sigma_{q\bar{q}}(x, z\mathbf{r}')] \\ &\quad - \Gamma_A[\mathbf{b}, \sigma_{q\bar{q}}(x, z\mathbf{r}' - \mathbf{r})] \cdot \Gamma_A[\mathbf{b}, \sigma_{q\bar{q}}(x, z\mathbf{r}')], \\ \Gamma_A[\mathbf{b}, \sigma_{gg}(x, z(\mathbf{r} - \mathbf{r}'))] &= 2\Gamma_A[\mathbf{b}, \sigma_{q\bar{q}}(x, z(\mathbf{r} - \mathbf{r}'))] - \Gamma_A^2[\mathbf{b}, \sigma_{q\bar{q}}(x, z(\mathbf{r} - \mathbf{r}'))]. \end{aligned} \quad (30)$$

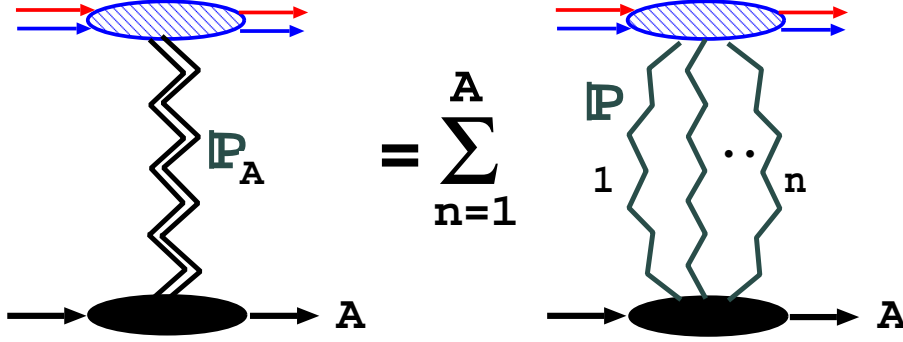


FIG. 6: (Color online) Exchange by a nuclear pomeron \mathbf{IP}_A in color dipole-nucleus scattering as a sum of multiple two-gluon pomeron exchanges.

Then after some algebra we obtain

$$\frac{(2\pi)^2 d\sigma_A(g^* \rightarrow Q\bar{Q})}{dzd^2pd^2\mathbf{b}} = S_{abs}(\mathbf{b}) \cdot \int d^2\boldsymbol{\kappa} \phi(\mathbf{b}, x_A, \boldsymbol{\kappa}) \left\{ |\Psi(z, \mathbf{p}) - \Psi(z, \mathbf{p} + z\boldsymbol{\kappa})|^2 + |\Psi(z, \mathbf{p} + \boldsymbol{\kappa}) - \Psi(z, \mathbf{p} + z\boldsymbol{\kappa})|^2 \right\} + \int d^2\boldsymbol{\kappa}_1 d^2\boldsymbol{\kappa}_2 \phi(\mathbf{b}, x_A, \boldsymbol{\kappa}_1) \phi(\mathbf{b}, x_A, \boldsymbol{\kappa}_2) |\Psi(z, \mathbf{p} + \boldsymbol{\kappa}_2) - \Psi(z, \mathbf{p} + z\boldsymbol{\kappa}_1 + z\boldsymbol{\kappa}_2)|^2. \quad (31)$$

One can associate with $\phi(\mathbf{b}, x_A, \boldsymbol{\kappa}_1)$ the exchange of a nuclear pomeron \mathbf{IP}_A which as indicated in Fig. 6 sums multiple exchanges of the pomeron \mathbf{IP} in interactions with nuclear targets ([2, 10], see also Sect. VIB). The first term is an exact counterpart of the free-nucleon result: in terms of the collective nuclear gluon density $\phi(\mathbf{b}, x_A, \boldsymbol{\kappa})$ it has exactly the same linear k_\perp -factorization form as the free nucleon result (24) in terms of $f(x_A, \boldsymbol{\kappa})$. As such it corresponds to the Kancheli-Mueller diagram of Fig. 7a. Despite the similarity of diagrams of Fig. 7a and Fig. 5d, the two inclusive spectra are different because $\mathbf{IP}_A \neq \mathbf{IP}$. Furthermore, this contribution to the nuclear spectrum is suppressed by the absorption factor $S_{abs}(\mathbf{b})$ and is entirely negligible for heavy nuclei. In this case only the second term survives, which is a manifestly nonlinear functional of the collective nuclear glue $\phi(\mathbf{b}, x_A, \boldsymbol{\kappa})$. It can be associated with the Kancheli-Mueller diagram of Fig. 7b. This completes our demonstration of the k_\perp -factorization breaking for single-jet spectra: the pattern of k_\perp -factorization changes from the conventional linear at the periphery of a nucleus to the nonlinear - quadratic - one for small impact

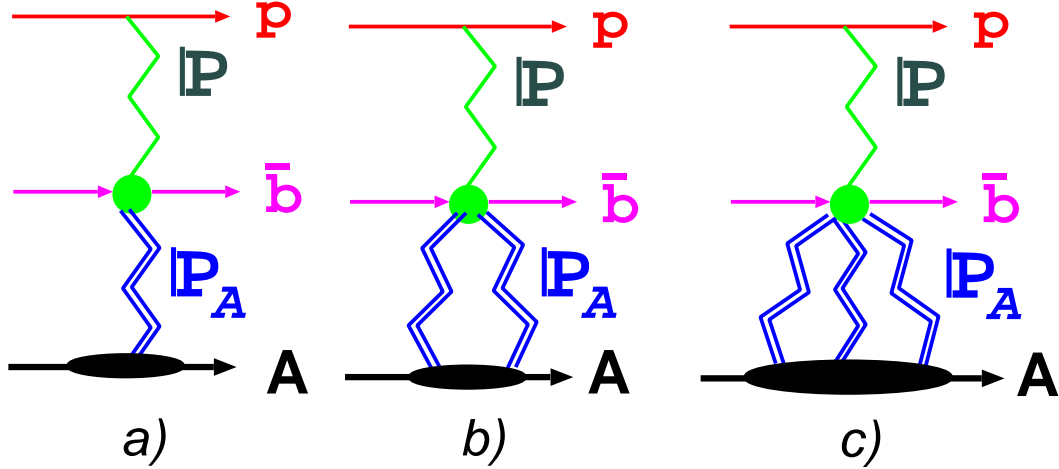


FIG. 7: (Color online) The Kancheli-Mueller diagrams for the mid-rapidity single-particle spectrum from gg subcollisions in pA collisions. The double-zigzag lines describe an exchange by the nuclear pomeron \mathbf{IP}_A . The open-charm spectrum in pp collisions is dominated by the diagram (a) with $\mathbf{IP}_A \rightarrow \mathbf{IP}$, see Fig. 5, the open charm spectrum in central pA collisions is dominated by the diagram (b) and the gluon jet production is dominated by the diagram (c).

parameters. In retrospect, the finding of linear k_{\perp} -factorization for the single quark jet spectrum in $\gamma^* \rightarrow q\bar{q}$ excitation can be traced back to the beam photon being colorless, by which the single-jet spectrum becomes an abelian observable [2]. In contrast to that, the origin of the nonlinear term in (31) is in the nonabelian nature of the 3-parton cross section (19), (29).

The z -dependence of the jet spectra enters through the wave-functions. To this end notice the strikingly different wave-function structure of the free-nucleon cross section (25) and its nuclear counterpart (31). This suggests a nontrivial dependence of the \mathbf{p} -spectra on the longitudinal variable z which will be different for the free-nucleon and nuclear targets. Vice versa, the z -distribution will vary with \mathbf{p} and the target mass number which can be called the LPM effect for open charm production.

VI. THE CRONIN EFFECT FOR OPEN CHARM

A. The charm p -distribution: nuclear vs. free nucleon targets

The impact of nonlinear k_{\perp} -factorization is quantified by the ratio of the free-nucleon and nuclear single-jet spectra,

$$R_{A/N}(z; x_A, \mathbf{p}) = \frac{d\sigma_A}{Ad\sigma_N}.$$

This ratio exhibits both shadowing, $R_{A/N}(z; x_A, \mathbf{p}) < 1$, and antishadowing, $R_{A/N}(z; x_A, \mathbf{p}) > 1$, properties, in the literature the latter is usually referred to as the Cronin effect. Our discussion of the Cronin effect is to a large extent based on the ideas and technique of the pQCD derivation of nuclear properties of the coherent diffractive breakup of pions into hard dijets [12, 13].

The principal points are best seen for central impact parameters, i.e., for $S_{abs}(\mathbf{b}) \rightarrow 0$:

$$\frac{(2\pi)^2 d\sigma_A(g^* \rightarrow Q\bar{Q})}{dzd^2\mathbf{p}d^2\mathbf{b}} = \int d^2\boldsymbol{\kappa}_1 d^2\boldsymbol{\kappa}_2 \phi(\mathbf{b}, x_A, \boldsymbol{\kappa}_1) \phi(\mathbf{b}, x_A, \boldsymbol{\kappa}_2) |\Psi(z, \mathbf{p} + \boldsymbol{\kappa}_2) - \Psi(z, \mathbf{p} + z\boldsymbol{\kappa}_1 + z\boldsymbol{\kappa}_2)|^2. \quad (32)$$

In all the comparisons of the free-nucleon and nuclear target observables we use the large- N_c approximation without further notice.

The results simplify greatly in two interesting cases. We start with the limit of slow quarks, $z \ll 1$, when the free nucleon spectrum becomes

$$\left. \frac{2(2\pi)^2 d\sigma_N(g^* \rightarrow Q\bar{Q})}{dzd^2\mathbf{p}} \right|_{z \ll 1} = \int d^2\boldsymbol{\kappa} f(x_A, \boldsymbol{\kappa}) |\Psi(z, \mathbf{p}) - \Psi(z, \mathbf{p} + \boldsymbol{\kappa})|^2. \quad (33)$$

In the limit of $z \ll 1$ the entire dependence of the nuclear spectrum (32) on $\boldsymbol{\kappa}_1$ is confined to the normalization integral $\int d^2\boldsymbol{\kappa}_1 \phi(\mathbf{b}, x_A, \boldsymbol{\kappa}_1) = 1 - S_{abs}(\mathbf{b})$ what lowers the nonlinearity of the nuclear cross section. Then, in conjunction with the linear term, $\propto S_{abs}(\mathbf{b})$, in (31), we find a result applicable at all impact parameters:

$$\left. \frac{(2\pi)^2 d\sigma_A(g^* \rightarrow Q\bar{Q})}{dzd^2\mathbf{p}d^2\mathbf{b}} \right|_{z \ll 1} = \int d^2\boldsymbol{\kappa} \phi(\mathbf{b}, x_A, \boldsymbol{\kappa}) |\Psi(z, \mathbf{p} + \boldsymbol{\kappa}) - \Psi(z, \mathbf{p})|^2. \quad (34)$$

We evidently recovered the linear k_{\perp} -factorization result (33), now in terms of the nuclear collective glue $\phi(\mathbf{b}, x_A, \boldsymbol{\kappa})$. The physics behind this finding is the above discussed abelianization of $g \rightarrow Q\bar{Q}$ at $z \ll 1$, by which it becomes equivalent to $\gamma^* \rightarrow Q\bar{Q}$.

The second simple result is found for leading quarks with $z \rightarrow 1$. Here the free-nucleon cross section again takes the form (33), whereas the nuclear single-jet spectrum can be cast in the convolution form

$$\left. \frac{d\sigma_A(g^* \rightarrow Q\bar{Q})}{dzd^2\mathbf{p}d^2\mathbf{b}} \right|_{z \rightarrow 1} = \int d^2\boldsymbol{\kappa} \phi(\mathbf{b}, x_A, \boldsymbol{\kappa}) \left. \frac{d\sigma_A(x, \mathbf{p} - \boldsymbol{\kappa})}{dzd^2\mathbf{p}d^2\mathbf{b}} \right|_{z \ll 1} + S_{abs}(\mathbf{b}) \left. \frac{d\sigma_A(x, \mathbf{p})}{dzd^2\mathbf{p}d^2\mathbf{b}} \right|_{z \ll 1}. \quad (35)$$

The leading term in (35) is a manifestly nonlinear - quadratic - functional of $\phi(\mathbf{b}, x_A, \boldsymbol{\kappa})$. Evidently, such a convolution would enhance the nuclear effects compared to the linear k_{\perp} -factorization formula (34). Arguably, when z varies from $z = 0$ to 1, the \mathbf{p} -dependence of the nuclear charm spectra shall interpolate between the ones given by equations (34) and (35).

B. Properties of the collective nuclear gluon density

The fundamental quantity of our formalism is the collective nuclear glue $\phi(\mathbf{b}, x_A, \boldsymbol{\kappa})$ per unit area in the impact parameter plane [2, 12, 13]. It is characterized by a new scale - the saturation scale,

$$Q_A^2(\mathbf{b}, x_A) \approx \frac{4\pi^2}{N_c} \alpha_S(Q_A^2) G(x_A, Q_A^2) T(\mathbf{b}), \quad (36)$$

a related quantity appears in other approaches to nuclear parton densities [35, 46]. At soft transverse momenta, $\boldsymbol{\kappa}^2 \lesssim Q_A^2(\mathbf{b}, x_A)$, the nuclear collective glue exhibits a plateau which signals the saturation of parton densities. A useful parameterization in the plateau region is

$$\phi(\mathbf{b}, x_A, \boldsymbol{\kappa}) \approx \frac{1}{\pi} \cdot \frac{Q_A^2(\mathbf{b}, x_A)}{(\boldsymbol{\kappa}^2 + Q_A^2(\mathbf{b}, x_A))^2}. \quad (37)$$

For hard gluons, $\boldsymbol{\kappa}^2 \gtrsim Q_A^2(\mathbf{b}, x_A)$, it is convenient to cite the unintegrated gluon density per bound nucleon:

$$f_A(\mathbf{b}, x_A, \boldsymbol{\kappa}) = \frac{\phi(\mathbf{b}, x_A, \boldsymbol{\kappa})}{\frac{1}{2}T(\mathbf{b})}$$

$$\begin{aligned}
&= f(x_A, \boldsymbol{\kappa}) \left[1 + \frac{\gamma^2}{2} \cdot \frac{\alpha_S(\boldsymbol{\kappa}^2)G(x_A, \boldsymbol{\kappa}^2)}{\alpha_S(Q_A^2)G(x_A, Q_A^2)} \cdot \frac{Q_A^2(\mathbf{b}, x_A)}{\boldsymbol{\kappa}^2} \right] \\
&= f(x_A, \boldsymbol{\kappa}) \left[1 + \frac{2\pi^2\gamma^2}{N_c\boldsymbol{\kappa}^2} \cdot \alpha_S(\boldsymbol{\kappa}^2)G(x_A, \boldsymbol{\kappa}^2)T(\mathbf{b}) \right] \\
&= f(x_A, \boldsymbol{\kappa}) [1 + \Delta_{HT}(\mathbf{b}, x_A, \boldsymbol{\kappa})] , \tag{38}
\end{aligned}$$

where $\gamma \approx 2$ is an exponent of the large- $\boldsymbol{\kappa}^2$ tail $f(x_A, \boldsymbol{\kappa}) \propto (\boldsymbol{\kappa}^2)^{-\gamma}$. Here we show explicitly the leading nuclear higher twist correction, $\Delta_{HT}(\mathbf{b}, x_A, \boldsymbol{\kappa})$, which gives rise to a nuclear antishadowing effect [2, 12, 13]. To this end, the saturated gluon density (37) can be regarded as a resummation of all higher twist terms $\sim (Q_A^2(\mathbf{b}, x_A)/\boldsymbol{\kappa}^2)^n$. Note the very strong nuclear suppression of the gluon density per bound nucleon $f_A(\mathbf{b}, x_A, \boldsymbol{\kappa})$ in the soft plateau region, $\boldsymbol{\kappa}^2 \lesssim Q_A^2(\mathbf{b}, x_A)$:

$$f_A(\mathbf{b}, x_A, \boldsymbol{\kappa}) \approx \frac{2}{\pi Q_A^2(\mathbf{b}, x_A)T(\mathbf{b})} \propto \frac{1}{T^2(\mathbf{b})} \propto A^{-2/3} \tag{39}$$

The explicit expansion for $\phi(\mathbf{b}, x_A, \boldsymbol{\kappa})$ in terms of the collective gluon density of j overlapping nucleons in the Lorentz-contracted nucleus [2, 12, 13] is

$$\phi(\mathbf{b}, x_A, \boldsymbol{\kappa}) = S_{abs}(\mathbf{b}) \sum_{j=1} \frac{1}{j!} \cdot \left(\frac{T(\mathbf{b})}{2} \right)^j \cdot f^{(j)}(x_A, \boldsymbol{\kappa}) \tag{40}$$

where $f^{(j)}(x, \boldsymbol{\kappa})$ is the j -fold convolution,

$$f^{(j)}(x, \boldsymbol{\kappa}) = \int \delta\left(\sum_{i=1}^j \boldsymbol{\kappa}_i - \boldsymbol{\kappa}\right) \prod_{i=1}^j f(x, \boldsymbol{\kappa}_i) d^2\boldsymbol{\kappa}_i. \tag{41}$$

Finally, we notice that $\phi(\mathbf{b}, x_A, \boldsymbol{\kappa})$ satisfies the important sum rule (see also [26, 33])

$$\int d^2\boldsymbol{\kappa} \boldsymbol{\kappa}^2 \left[\phi(\mathbf{b}, x_A, \boldsymbol{\kappa}) - \frac{1}{2}T(\mathbf{b})f(x_A, \boldsymbol{\kappa}) \right] = 0, \tag{42}$$

which readily follows from the property that $\Gamma_A[\mathbf{b}, \sigma(x, \mathbf{r})] - \frac{1}{2}T(\mathbf{b})\sigma(x, \mathbf{r})$ vanishes $\propto \sigma^2(x, \mathbf{r})$ as $\mathbf{r}^2 \rightarrow 0$. The effect of nuclear suppression for nuclear soft gluons, see eqs. (37) and (39), is compensated for by nuclear antishadowing (38) for hard glue.

The familiar integrated gluon density equals

$$G(x, Q^2) = \frac{N_c}{4\pi^2\alpha_S} \int^{Q^2} d^2\boldsymbol{\kappa} \boldsymbol{\kappa}^2 f(x, \boldsymbol{\kappa}) \tag{43}$$

its nuclear counterpart per bound nucleon, $G_A(\mathbf{b}, x_A, \kappa^2)$, can be defined likewise in terms of $f_A(\mathbf{b}, x_A, \kappa)$. Then the corollary of the sum rule (42) is that for $Q^2 \gg Q_A^2(\mathbf{b}, x_A)$

$$\begin{aligned}
G_A(\mathbf{b}, x_A, Q^2) - G(\mathbf{b}, x_A, Q^2) &= - \int_{Q^2} d^2\kappa \kappa^2 f(x_A, \kappa) \Delta_{HT}(\mathbf{b}, x_A, \kappa) \\
&\approx - \frac{2\gamma^2\pi^2\alpha_S(Q^2)}{N_c} \cdot \frac{\alpha_S(Q^2)G(x_A, Q^2)}{\alpha_S(Q_A^2(\mathbf{b}, x_A))G(x_A, Q_A^2(\mathbf{b}, x_A))} \cdot \frac{Q_A^2(\mathbf{b}, x_A)}{Q^2} \cdot \frac{\partial G(x_A, Q^2)}{\partial \log Q^2} \\
&\approx - \frac{\gamma^2\pi^2\alpha_S(Q^2)}{N_c} \cdot \frac{\alpha_S(Q^2)Q_A^2(\mathbf{b}, x_A)}{\alpha_S(Q_A^2(\mathbf{b}, x_A))G(x_A, Q_A^2(\mathbf{b}, x_A))} \cdot \frac{\partial G^2(x_A, Q^2)}{\partial Q^2}, \tag{44}
\end{aligned}$$

where we made use of the expansion (38).

C. The Cronin effect: nuclear shadowing for $p^2 \lesssim Q_A^2(\mathbf{b}, x_A)$

For the sake of illustration we start with the case of $z \ll 1$ and assume that the saturation scale is so large that even for $m_Q^2 \ll p^2 \ll Q_A^2(\mathbf{b}, x_A)$ the jets are still perturbatively hard. Because the dominant contribution to (34) comes from $\kappa^2 \sim Q_A^2(\mathbf{b}, x_A)$, the expansion (B.6) of Appendix B simplifies further, and the κ integration can be carried out explicitly

$$\begin{aligned}
\left. \frac{(2\pi)^2 d\sigma_A(g^* \rightarrow Q\bar{Q})}{dz d^2p d^2\mathbf{b}} \right|_{z \ll 1} &= 2T_F\alpha_S \cdot \frac{1}{p^2} \int d^2\kappa \phi(\mathbf{b}, x_A, \kappa) \\
&= [1 - S_{abs}(\mathbf{b})] \cdot 2T_F\alpha_S \cdot \frac{1}{p^2}. \tag{45}
\end{aligned}$$

It is entirely dominated by the contribution from $\kappa^2 \gtrsim p^2$, which in the language of evolution amounts to the anti-DGLAP splitting of collective nuclear gluons with large transverse momentum κ into quarks with small transverse momentum p .

The integration over all impact parameters gives

$$2 \int d^2\mathbf{b} [1 - S_{abs}(\mathbf{b})] = 2 \int d^2\mathbf{b} \left\{ 1 - \exp \left[-\frac{1}{2} \sigma_0(x_A) T(\mathbf{b}) \right] \right\} = \sigma_A[\sigma_0(x_A)], \tag{46}$$

which is the familiar Glauber-Gribov nuclear total cross section $\sigma_A[\sigma_0]$ for a projectile with the free-nucleon cross section σ_0 , and

$$R_{A/N}(z; x_A, \mathbf{p}) = \frac{\sigma_A[\sigma_0(x_A)]}{A\sigma_0(x_A)} \sim A^{-1/3} < 1 \tag{47}$$

A marginal caveat is that for the fixed quark-jet momentum the inequality $\mathbf{p}^2 \ll Q_A^2(\mathbf{b}, x_A)$ does not hold uniformly over all impact parameters \mathbf{b} , it breaks down for the most peripheral interactions, the peripheral contribution does not affect the shadowing property $R_{A/N}(z; x_A, \mathbf{p}) < 1$, though.

Now turn to the opposite limit of $z \rightarrow 1$. Here the free-nucleon cross section is the same as for $z \ll 1$. The convolution representation (35) for the nuclear spectrum is already suggestive of stronger nuclear effects. The analysis by the straightforward use of (32) in which one can neglect \mathbf{p} in the arguments of the wave functions is still simpler:

$$\left. \frac{(2\pi)^2 d\sigma_A(g^* \rightarrow Q\bar{Q})}{dz d^2\mathbf{p} d^2\mathbf{b}} \right|_{z \rightarrow 1} = 2T_F \alpha_S \int d^2\boldsymbol{\kappa}_1 d^2\boldsymbol{\kappa}_2 \phi(\mathbf{b}, x_A, \boldsymbol{\kappa}_1) \phi(\mathbf{b}, x_A, \boldsymbol{\kappa}_2) \frac{\boldsymbol{\kappa}_1^2}{(\boldsymbol{\kappa}_2^2 + m_Q^2)((\boldsymbol{\kappa}_1 + \boldsymbol{\kappa}_2)^2 + m_Q^2)}. \quad (48)$$

The integral in the r.h.s. will be dominated by the two logarithmic contributions from (i) $\boldsymbol{\kappa}_2^2 \ll \boldsymbol{\kappa}_1^2$ and (ii) $(\boldsymbol{\kappa}_2 + \boldsymbol{\kappa}_1)^2 \ll \boldsymbol{\kappa}_1^2$:

$$\begin{aligned} & \int d^2\boldsymbol{\kappa}_1 d^2\boldsymbol{\kappa}_2 \phi(\mathbf{b}, x_A, \boldsymbol{\kappa}_1) \phi(\mathbf{b}, x_A, \boldsymbol{\kappa}_2) \frac{\boldsymbol{\kappa}_1^2}{(\boldsymbol{\kappa}_2^2 + m_Q^2)((\boldsymbol{\kappa}_1 + \boldsymbol{\kappa}_2)^2 + m_Q^2)} \\ & \approx \pi \int d^2\boldsymbol{\kappa}_1 \left[\phi(\mathbf{b}, x_A, \boldsymbol{\kappa}_1) \phi(\mathbf{b}, x_A, 0) + \phi^{(2)}(\mathbf{b}, x_A, \boldsymbol{\kappa}_1) \right] \log \frac{\boldsymbol{\kappa}_1^2}{m_Q^2} \\ & \approx \pi [\phi(\mathbf{b}, x_A, 0) + \phi^{(2)}(\mathbf{b}, x_A, 0)] \log \frac{Q_A^2(\mathbf{b}, x_A)}{m_Q^2} \end{aligned} \quad (49)$$

where $\phi^{(2)}(\mathbf{b}, x_A, \boldsymbol{\kappa})$ is the convolution

$$\phi^{(2)}(\mathbf{b}, x_A, \boldsymbol{\kappa}) = (\phi \otimes \phi)(\mathbf{b}, x_A, \boldsymbol{\kappa}). \quad (50)$$

For heavy nuclei $\phi^{(2)}(\mathbf{b}, x_A, \boldsymbol{\kappa})$ has the same meaning as $\phi(\mathbf{b}, x_A, \boldsymbol{\kappa})$ but for twice larger $T(\mathbf{b})$, what counts for the purposes of the present discussion is that

$$[\phi(\mathbf{b}, x_A, 0) + \phi^{(2)}(\mathbf{b}, x_A, 0)] \approx \frac{1}{\pi Q_A^2(\mathbf{b}, x_A)} \propto A^{-1/3} \quad (51)$$

The final result for the nuclear spectrum at $z \rightarrow 1$ is

$$\left. \frac{(2\pi)^2 d\sigma_A(g^* \rightarrow Q\bar{Q})}{dz d^2\mathbf{p} d^2\mathbf{b}} \right|_{z \rightarrow 1} \approx \frac{2T_F \alpha_S (Q_A^2(\mathbf{b}, x_A))}{Q_A^2(\mathbf{b}, x_A)} \cdot \log \frac{Q_A^2(\mathbf{b}, x_A)}{m_Q^2} \quad (52)$$

The first dramatic effect is that the \mathbf{p} -spectrum of fast quarks will be flat for $\mathbf{p}^2 \lesssim Q_A^2(\mathbf{b}, x_A)$ which must be contrasted to the $\propto 1/\mathbf{p}^2$ free-nucleon spectrum (45). The second dramatic effect is a strong enhancement of the shadowing effect. The result of the impact parameter integration can be evaluated as

$$\pi \int d^2\mathbf{b} [\phi(\mathbf{b}, x_A, 0) + \phi^{(2)}(\mathbf{b}, x_A, 0)] \approx \frac{\sigma_A[\sigma_0(x_A)]}{\langle Q_A^2(\mathbf{b}, x_A) \rangle} \quad (53)$$

where $\langle Q_A^2(\mathbf{b}, x_A) \rangle$ is an average saturation scale. This gives the shadowing effect

$$R_{A/N}(z \rightarrow 1; x_A, \mathbf{p}) \approx \frac{\sigma_A[\sigma_0(x_A)]}{A\sigma_0(x_A)} \cdot \frac{\mathbf{p}^2}{\langle\langle Q_A^2(\mathbf{b}, x_A) \rangle\rangle} \cdot \log \frac{Q_A^2(\mathbf{b}, x_A)}{m_Q^2} \propto A^{-2/3}. \quad (54)$$

The analytic formula for the transition from small to large z can be worked out making use of the explicit parameterization (36). The gross features of this transition are well reproduced by the interpolation formula

$$R_{A/N}(z; x_A, \mathbf{p}) \approx \frac{\sigma_A[\sigma_0(x_A)]}{A\sigma_0(x_A)} \left[\frac{\mathbf{p}^2}{\mathbf{p}^2 + z^2 \langle Q_A^2(\mathbf{b}, x_A) \rangle} + \frac{z^2 \mathbf{p}^2}{\langle Q_A^2(\mathbf{b}, x_A) \rangle} \cdot \log \frac{\langle Q_A^2(\mathbf{b}, x_A) \rangle}{m_Q^2} \right] \quad (55)$$

applicable for $\mathbf{p}^2 \lesssim \langle Q_A^2(\mathbf{b}, x_A) \rangle$.

D. The Cronin effect: hard quark-jets, $\mathbf{p}^2 \gtrsim Q_A^2(\mathbf{b}, x_A)$

1. Open charm from the direct and resolved gluon interactions

The above k_\perp -factorization formulas are exact and can be directly applied to the calculation of the jet spectra. In order to make a contact with the more familiar treatment of photoproduction of jets, here we present the LL \mathbf{p}^2 decomposition of the jet spectra into the direct and resolved interactions of the incident parton a . Such a decomposition will make more obvious the origin of the Cronin effect, although in the practical calculations there is no need to resort to the LL \mathbf{p}^2 approximation.

For hard jets we can use the large- \mathbf{p} approximation (B.6) of Appendix B. Then the hard single-jet spectrum for the free-nucleon target takes the form

$$\frac{d\sigma_N(g^* \rightarrow Q\bar{Q})}{dzd^2\mathbf{p}} =$$

$$\frac{T_F\alpha_S(\mathbf{p}^2)[z^2 + (1-z)^2]}{(2\pi)^2} \int d^2\boldsymbol{\kappa} \boldsymbol{\kappa}^2 f(x_A, \boldsymbol{\kappa}) \cdot \left[\frac{z^2}{\mathbf{p}^2} + \frac{(1-z)^2}{(\mathbf{p} + \boldsymbol{\kappa})^2} \right] \cdot \frac{1}{(\mathbf{p} + z\boldsymbol{\kappa})^2}, \quad (56)$$

whereas for the heavy nuclear target

$$\begin{aligned} \frac{d\sigma_A(g^* \rightarrow Q\bar{Q})}{dzd^2\mathbf{p}d^2\mathbf{b}} &= \frac{2T_F\alpha_S(\mathbf{p}^2)[z^2 + (1-z)^2]}{(2\pi)^2} \\ &\times \int d^2\boldsymbol{\kappa}_1 d^2\boldsymbol{\kappa}_2 \phi(\mathbf{b}, x_A, \boldsymbol{\kappa}_1) \phi(\mathbf{b}, x_A, \boldsymbol{\kappa}_2) \frac{(z\boldsymbol{\kappa}_1 - (1-z)\boldsymbol{\kappa}_2)^2}{(\mathbf{p} + \boldsymbol{\kappa}_2)^2 (\mathbf{p} + z\boldsymbol{\kappa}_1 + z\boldsymbol{\kappa}_2)^2}. \end{aligned} \quad (57)$$

For the sake of brevity here we suppressed the contribution from the linear term $\propto S_{abs}(\mathbf{b})$ in (31).

In the spirit of LL \mathbf{p}^2 one can disentangle two distinct sources of the transverse momentum of the quark-jet. In the first case the pQCD subprocess can be viewed as the large- \mathbf{p} direct (unresolved) boson-gluon fusion $g^*g \rightarrow Q\bar{Q}$ where the exchanged gluon g has a small transverse momentum $|\boldsymbol{\kappa}| \lesssim |\mathbf{p}|$, the large \mathbf{p} flows in the t -channel of the pQCD subprocess $g^*g \rightarrow Q\bar{Q}$. Such a contribution can be evaluated as

$$\begin{aligned} \left. \frac{d\sigma_N(g^* \rightarrow Q\bar{Q})}{dzd^2\mathbf{p}} \right|_{dir} &= \frac{T_F\alpha_S(\mathbf{p}^2)[z^2 + (1-z)^2]^2}{(\mathbf{p}^2)^2} \int^{\mathbf{p}^2} d^2\boldsymbol{\kappa} \boldsymbol{\kappa}^2 f(x_A, \boldsymbol{\kappa}) \\ &= \frac{T_F\alpha_S(\mathbf{p}^2)[z^2 + (1-z)^2]^2}{(\mathbf{p}^2)^2} \cdot \frac{4\pi^2\alpha_S(\mathbf{p}^2)}{N_c} \cdot G(x_A, \mathbf{p}^2) \\ &= \frac{2\pi[z^2 + (1-z)^2]}{\mathbf{p}^2} \cdot \frac{4\pi^2\alpha_S(\mathbf{p}^2)}{N_c} \cdot \frac{dQ(z, \mathbf{p})}{d\mathbf{p}^2} \cdot G(x_A, \mathbf{p}^2). \end{aligned} \quad (58)$$

First, one recovers the familiar collinear factorization proportionality to the target gluon density $G(x_A, \mathbf{p}^2)$. Second, one readily identifies the unintegrated density of large- \mathbf{p} quarks in the gluon,

$$\frac{dQ(z, \mathbf{p})}{d\mathbf{p}^2} = \frac{T_F\alpha_S(\mathbf{p}^2)[z^2 + (1-z)^2]}{2\pi\mathbf{p}^2}. \quad (59)$$

One can say that the direct process probes the transverse momentum distribution of quarks in the beam gluon g^* .

The second contribution corresponds to the t -channel quark being close to the mass shell, $(\mathbf{p} + \boldsymbol{\kappa})^2 \sim m_Q^2$. In this case the large transverse momentum \mathbf{p} of the quark-jet comes from the large transverse momentum of the exchanged gluon, $\boldsymbol{\kappa} \approx -\mathbf{p}$, in close

similarity to the pomeron splitting mechanism for production of hard diffractive dijets [47]. It also can be viewed as a jet from the resolved gluon interactions. All the target information is encoded in the unintegrated $f(x_A, \boldsymbol{\kappa})$ for a free nucleon or $\phi(\mathbf{b}, x_A, \mathbf{p})$ for a nucleus, and the process itself looks as the fusion $Qg \rightarrow Q'$. One must be careful with the fusion reinterpretation as the resolved contribution is only a part of the more generic $g^*g \rightarrow Q\bar{Q}$ and singling it out only makes a unique sense to the LL \mathbf{p}^2 approximation.

The case of finite $0 < z < 1$ is a bit more involved and will be considered to more detail elsewhere. The two poles in (56), at $(\mathbf{p} + z\boldsymbol{\kappa})^2 = 0$ and $(\mathbf{p} - \boldsymbol{\kappa})^2 = 0$, are well separated. At $z \rightarrow 1$ the two poles merge but the residue vanishes $\propto (1-z)^2$. Here-below for the sake of illustration we focus on slow quark production, $z \ll 1$. For the massive quarks upon the azimuthal averaging

$$\left\langle \frac{1}{(\mathbf{p} - \boldsymbol{\kappa})^2 + m_Q^2} \right\rangle \Rightarrow \frac{1}{\sqrt{(\mathbf{p}^2 - \boldsymbol{\kappa}^2 - m_Q^2)^2 + 4\mathbf{p}^2 m_Q^2}} \Rightarrow \frac{1}{|\mathbf{p}^2 - \boldsymbol{\kappa}^2| + \delta^2}, \quad (60)$$

where the infrared regulator of the $d\boldsymbol{\kappa}^2$ integration can be taken as $\delta^4 \approx \mathbf{p}^2 m_Q^2$. The corresponding contribution to the quark-jet cross section for the free-nucleon target can be evaluated as

$$\begin{aligned} \left. \frac{d\sigma_N(g^* \rightarrow Q\bar{Q})}{dz d^2\mathbf{p}} \right|_{res} &\approx \frac{T_F \pi \alpha_S(\mathbf{p}^2)}{(2\pi)^2} f(x_A, \mathbf{p}) \log \frac{\mathbf{p}^2}{m_Q^2} \\ &= \frac{2\pi}{\mathbf{p}^2} \cdot \frac{4\pi^2 \alpha_S(\mathbf{p}^2)}{N_c} \cdot \frac{dG(x_A, \mathbf{p}^2)}{d\mathbf{p}^2} \cdot Q(z \ll 1, \mathbf{p}). \end{aligned} \quad (61)$$

The emerging logarithm times the splitting function can be identified with the integrated quark structure function $Q(z \ll 1, \mathbf{p}^2)$ of the beam gluon g^* probed by the exchanged gluon g of virtuality $Q_g^2 = \mathbf{p}^2$. The resolved gluon mechanism probes the transverse momentum distribution of gluons in the target.

In the more general case one must take the quark density $Q(x_B, \mathbf{p}^2)$ where x_B is the fraction of the lightcone momentum of the beam carried by the quark Q . Combining together (58) and (61) we find the spectrum of hard quark-jets which is proportional to

$$\left(\frac{dQ(x_B, \mathbf{p}^2)}{d\mathbf{p}^2} G(x_A, \mathbf{p}^2) + Q(x_B, \mathbf{p}^2) \frac{dG(x_A, \mathbf{p}^2)}{d\mathbf{p}^2} \right) = \frac{d}{d\mathbf{p}^2} [Q(x_B, \mathbf{p}^2) G(x_A, \mathbf{p}^2)], \quad (62)$$

which restores the beam-target symmetry. A similar observation has been made in [26]. The last form shows that in the general case the both mechanisms are of comparable importance. It also demonstrates the nonlocality properties of the $\bar{b}\mathbf{IP}\bar{b}\mathbf{IP}$ vertex in the Kancheli-Mueller diagram of Fig. 5d. The derivation of the nuclear counterparts of (58) and (61) for $z \ll 1$ is straightforward and need not be repeated here. We proceed directly to the derivation of the Cronin effect.

2. *Antishadowing property of collective nuclear gluon density as an origin of the Cronin effect*

For a more accurate isolation of the Cronin effect for hard jets consider the nuclear excess cross section

$$\frac{d\Delta\sigma_A}{d^2\mathbf{b}} = \frac{d\sigma_A}{d^2\mathbf{b}} - \frac{1}{2}T(\mathbf{b})d\sigma_N. \quad (63)$$

Again we start with $z \ll 1$. Suppressing common factors and making use of (60) we need to evaluate

$$\frac{d\Delta\sigma_A}{dzd^2\mathbf{p}d\mathbf{b}} \propto \int d^2\boldsymbol{\kappa} \frac{\boldsymbol{\kappa}^2}{|\mathbf{p}^2 - \boldsymbol{\kappa}^2| + \delta^2} [\phi(\mathbf{b}, x_A, \boldsymbol{\kappa}) - \frac{1}{2}T(\mathbf{b})f(x_A, \boldsymbol{\kappa})] \quad (64)$$

A priori the sign of this quantity is not obvious because the function $\Delta\phi_A(\mathbf{b}, x_A, \boldsymbol{\kappa}) = \phi(\mathbf{b}, x_A, \boldsymbol{\kappa}) - \frac{1}{2}T(\mathbf{b})f(x_A, \boldsymbol{\kappa})$ is negative valued for $\boldsymbol{\kappa}^2 \lesssim Q_A^2(x_A, \mathbf{b})$ and positive valued in the antishadowing region described by eq. (57). We decompose $\boldsymbol{\kappa}^2/(|\mathbf{p}^2 - \boldsymbol{\kappa}^2| + \delta^2)$ as follows:

$$\frac{\boldsymbol{\kappa}^2}{|\mathbf{p}^2 - \boldsymbol{\kappa}^2| + \delta^2} = \theta(\mathbf{p}^2 - \boldsymbol{\kappa}^2) \cdot \frac{\boldsymbol{\kappa}^2}{\mathbf{p}^2} + \theta(\boldsymbol{\kappa}^2 - \mathbf{p}^2) + K(\mathbf{p}^2, \boldsymbol{\kappa}^2). \quad (65)$$

Here the first term isolates the direct boson-fusion contribution, whereas the collinear quark-pole contribution is contained entirely in $K(\mathbf{p}^2, \boldsymbol{\kappa}^2)$ which can readily be shown to be a positive-valued function which vanishes $\sim \kappa^4$ for $\boldsymbol{\kappa}^2 \ll \mathbf{p}^2$ and $\sim 1/\boldsymbol{\kappa}^2$ for $\boldsymbol{\kappa}^2 \gg \mathbf{p}^2$.

The shadowing effect from the negative-valued $\Delta\phi_A(\mathbf{b}, x_A, \boldsymbol{\kappa})$ at small $\boldsymbol{\kappa}^2 \lesssim Q_A^2(\mathbf{b}, x_A)$ is concentrated in the contribution from the first term in (65) which by virtue of the sum

rule (41) can be represented as

$$\frac{1}{\mathbf{p}^2} \int_0^{\mathbf{p}^2} d\boldsymbol{\kappa}^2 \boldsymbol{\kappa}^2 \Delta\phi_A(\mathbf{b}, x_A, \boldsymbol{\kappa}) = -\frac{1}{\mathbf{p}^2} \int_{\mathbf{p}^2}^{\infty} d\boldsymbol{\kappa}^2 \boldsymbol{\kappa}^2 \Delta\phi_A(\mathbf{b}, x_A, \boldsymbol{\kappa}). \quad (66)$$

Consequently, the nuclear excess cross section is entirely calculable in terms of gluon densities in the hard region of $\boldsymbol{\kappa}^2 \gtrsim \mathbf{p}^2$:

$$\begin{aligned} \mathbf{p}^2 \frac{d\Delta\sigma_A}{dzd^2\mathbf{p}d\mathbf{b}} &\propto -\frac{1}{\mathbf{p}^2} \int_{\mathbf{p}^2}^{\infty} d\boldsymbol{\kappa}^2 \boldsymbol{\kappa}^2 \Delta\phi_A(\mathbf{b}, x_A, \boldsymbol{\kappa}) \\ &+ \int_{\mathbf{p}^2}^{\infty} d\boldsymbol{\kappa}^2 \Delta\phi_A(\mathbf{b}, x_A, \boldsymbol{\kappa}) \\ &+ \frac{1}{\pi} \int d^2\boldsymbol{\kappa} K(\mathbf{p}^2, \boldsymbol{\kappa}^2) \Delta\phi_A(\mathbf{b}, x_A, \boldsymbol{\kappa}) \end{aligned} \quad (67)$$

Now notice that in this hard region $\Delta\phi_A(\mathbf{b}, x_A, \boldsymbol{\kappa}) \propto 1/(\boldsymbol{\kappa}^2)^3$, see eq. (38), and all integrals in (67) are well converging ones. The collinear quark-pole contribution can be evaluated as it was done in (61), factoring out $\mathbf{p}^2 \Delta\phi_A(\mathbf{b}, \mathbf{p})$, so that to logarithmic accuracy

$$\mathbf{p}^2 \frac{d\Delta\sigma_A}{dzd^2\mathbf{p}d\mathbf{b}} \propto \Delta\phi_A(\mathbf{b}, \mathbf{p}) \left[-1 + \frac{1}{2} + \log \frac{\mathbf{p}^2}{m_Q^2} \right]. \quad (68)$$

Following the derivation of eq. (61) we can associate $\log(\mathbf{p}^2/m_Q^2)$ with $Q(z \ll 1, \mathbf{p})$ and to LL \mathbf{p}^2 accuracy

$$\begin{aligned} \frac{d\Delta\sigma_A}{dzd^2\mathbf{p}d\mathbf{b}} &= \frac{d\sigma_N}{dzd^2\mathbf{p}} \Big|_{res} \cdot T(\mathbf{b}) \cdot \left[\frac{f_A(\mathbf{b}, x_A, \mathbf{p}^2)}{f(x_A, \mathbf{p}^2)} - 1 \right] \\ &= \frac{d\sigma_N}{dzd^2\mathbf{p}} \Big|_{res} \cdot T(\mathbf{b}) \Delta_{HT}(\mathbf{b}, x_A, \mathbf{p}). \end{aligned} \quad (69)$$

The result for the resolved interactions does not depend on the projectile parton a ,

$$[R_{A/N}(z \ll 1; x_A, \mathbf{p}) - 1]_{res} = \Delta_{HT}(\mathbf{b}, x_A, \mathbf{p}). \quad (70)$$

while the dilution of the Cronin effect by the contribution from direct interactions to the free-nucleon is process dependent:

$$R_{A/N}(z \ll 1; x_A, \mathbf{p}) - 1 = \frac{d\sigma_N(res)}{d\sigma_N(res) + d\sigma_N(dir)} \cdot [R_{A/N}(z \ll 1; x_A, \mathbf{p}) - 1]_{res}. \quad (71)$$

Hereafter we focus on the projectile independent antishadowing for resolved interaction and suppress the subscript 'res'. For heavy nuclei

$$\int d^2\mathbf{b} T^2(\mathbf{b}) \approx \frac{9A^2}{8\pi R_A^2} \quad (72)$$

and we obtain our final estimate for the antishadowing Cronin effect at large- \mathbf{p}^2

$$\Delta_{Qg}(z \ll 1; x_A, \mathbf{p}) = R_{A/N}(z \ll 1; x_A, \mathbf{p}) - 1 \approx \frac{9\pi\gamma^2}{4N_c} \cdot \frac{\alpha_S(\mathbf{p}^2) \cdot G(x_A, \mathbf{p}^2)}{\mathbf{p}^2} \cdot \frac{A}{R_A^2}. \quad (73)$$

Here we adopted the same subscript Qg as in the familiar splitting functions.

First, of the two components the direct g^*g -fusion would have given nuclear shadowing, see the first line in eq. (67), the antishadowing nuclear excess cross section is a feature of the resolved gluon interactions. Second, the fundamental point is that for hard jets the nuclear excess cross section follows directly from the nuclear antishadowing component $\Delta_{HT}(\mathbf{b}, x_A, \mathbf{p})$ of the collective nuclear gluon density [12, 13]. Third, the antishadowing rises with the nuclear mass number, $R_{A/N}(z; x_A, \mathbf{p}) - 1 \propto A^{1/3}$. Fourth, the antishadowing nuclear excess is a special quadratic functional of the gluon density in the proton - a product of the integrated and unintegrated gluon densities. Finally, for hard jets the antishadowing Cronin effect vanishes $\propto 1/p^2$. Whereas the antishadowing for hard jets, $R_{A/N}(z; x_A, \mathbf{p}) > 1$, has been discussed by many authors under model assumptions and specific parameterizations for the dipole cross section/unintegrated glue (e.g. [24–26, 33] and references therein), the above reported model independent derivation, and identification of the source, of antishadowing Cronin effect are new results.

3. Variations of the Cronin effect from slow to leading charm

The convolution representation (35) makes it obvious that the above findings on the Cronin effect are directly applicable to the opposite limiting case of $z \rightarrow 1$ as well. We recall that the free-nucleon spectra for $z \rightarrow 1$ and $z \ll 1$ are identical. The smearing of the decreasing spectrum (34) does obviously enhance the antishadowing effect at large \mathbf{p} which can readily be seen as follows. The \mathbf{p} -dependence of the spectra (58) and (61) is

driven by the factor $1/(\mathbf{p}^2)^2$ and the enhancement of the Cronin effect will for the most part be due to the smearing of $1/[(\mathbf{p} - \boldsymbol{\kappa})^2]^2$ in (35). The large- \mathbf{p} expansion

$$\frac{1}{[(\mathbf{p} - \boldsymbol{\kappa})^2]^2} \Rightarrow \frac{1}{(\mathbf{p}^2)^2} \left[1 + 4 \frac{\boldsymbol{\kappa}^2}{\mathbf{p}^2} \right], \quad (74)$$

in which the azimuthal averaging is understood, gives an enhancement of $R_{A/N}(z \ll 1; x_A, \mathbf{p})$ by the extra factor

$$\begin{aligned} \rho_{A/N}(\mathbf{p}) &= \int d^2 \boldsymbol{\kappa} \phi(\mathbf{b}, x_A, \boldsymbol{\kappa}) \left[1 + 4 \frac{\boldsymbol{\kappa}^2}{\mathbf{p}^2} \right] \\ &= 1 + 2 \frac{\alpha_S(\mathbf{p}^2) G(x_A, \mathbf{p}^2)}{\alpha_S(Q_A^2) G(x_A, Q_A^2)} \cdot \frac{Q_A^2(\mathbf{b}, x_A)}{\mathbf{p}^2} \approx 1 + \Delta_{HT}(\mathbf{b}, x_A, \mathbf{p}), \end{aligned} \quad (75)$$

cf. eq. (38) for $\gamma \approx 2$. Consequently, at $z \rightarrow 1$ the antishadowing Cronin effect will be twice stronger than that at $z \ll 1$,

$$\Delta_{Qg}(z \rightarrow 1; x_A, \mathbf{p}) = R_{A/N}(z \ll 1; x_A, \mathbf{p}) \cdot \rho_{A/N}(\mathbf{p}) - 1 \approx 2\Delta_{Qg}(z \ll 1; x_A, \mathbf{p}), \quad (76)$$

what nicely correlates with the stronger nuclear shadowing at small \mathbf{p} . The same correlation is obvious from the sum rule which relates the \mathbf{p} -integrated nuclear cross sections for $z \rightarrow 1$ and $z \ll 1$,

$$\left. \frac{d\sigma_A(g^* \rightarrow Q\bar{Q})}{dzd^2\mathbf{b}} \right|_{z \rightarrow 1} = \left. \frac{d\sigma_A(g^* \rightarrow Q\bar{Q})}{dzd^2\mathbf{b}} \right|_{z \ll 1}, \quad (77)$$

which readily follows from the convolution representation (35).

4. Numerical estimates for the Cronin effect

The antishadowing properties of the collective nuclear gluon density have been studied [12, 13] in connection with the A -dependence of coherent diffractive dijet production. The starting point was the unintegrated gluon density in the proton, $f(x, \boldsymbol{\kappa})$, adjusted to reproduce the $\gamma^* N$ interactions from real photoproduction, $Q^2 = 0$, to DIS at large Q^2 [14]. The quantity of interest is the antishadowing higher twist effect in the collective nuclear gluon density for j overlapping nucleons which is given by the j -fold convolution $f^{(j)}(x_A, \boldsymbol{\kappa})$. This density per overlapping nucleon was represented in ref. [12] as

$$f_A(\mathbf{b}, x_A, \boldsymbol{\kappa}) = \frac{f^{(j)}(x_A, \boldsymbol{\kappa})}{j\sigma_0^{j-1}} = f(x_A, \boldsymbol{\kappa}) [1 + (j-1)\Delta_j(x_A, \boldsymbol{\kappa})]. \quad (78)$$

With reference to the Poissonian form of the multiple scattering expansion (40), in Figs. 8,9 we show $\Delta_{Cronin}(x_A, \boldsymbol{\kappa}) = j \cdot \Delta_j(x_A, \boldsymbol{\kappa})$ for two values of x_A .

These results for $\Delta_{Cronin}(x_A, \boldsymbol{\kappa})$ can be used to evaluate $\Delta(x_A, \mathbf{p}) = R_{A/N}(x_A, \mathbf{p}) - 1$ for different jet production subprocesses and for different nuclei:

$$\Delta_{Qg}(z \ll 1; x_A, \mathbf{p}) \approx \Delta_{Cronin}(x_A, \boldsymbol{\kappa}) \Big|_{j \approx \langle j \rangle} \quad (79)$$

For the ^{196}Pt nucleus, which is not any different from gold - the favorite of RHIC, the average value of j in the expansion (40) is $\langle j \rangle \approx 4$. At $x_A = 0.01$ the peak value of the antishadowing effect, $\Delta_{Qg}(z \ll 1; x_A, \mathbf{p}) \approx 0.7$, will be reached at $p \approx (2 \div 2.5)$ GeV. It is important that although the numerical studies in [2] suggest not so large $Q_A^2 \lesssim 1$ GeV², the peak of the antishadowing effect is placed at transverse momenta p which are sufficiently large to justify the pQCD evaluations. For quark jets with $z \rightarrow 1$ the antishadowing effect will be twice stronger. The relationship between $\Delta_{Cronin}(x_A, \boldsymbol{\kappa})$ and $\Delta_{gg}(z; x_A, \mathbf{p})$, $\Delta_{gq}(z; x_A, \mathbf{p})$ for gluon jets will be discussed in Sections VII B and VIII B, respectively.

The x_A -dependence of the Cronin effect is noteworthy. At $x_A = 0.001$ the peak value of the antishadowing effect, $\Delta_{Qg}(z \ll 1; x_A, \mathbf{p}) \approx 0.25$, will be reached at $p \approx (3 \div 3.5)$ GeV. This x -dependence of the position and magnitude of the peak value of the antishadowing effect is driven by three effects. The first one is the x -dependence of $Q_A^2(x, \mathbf{b})$ which is similar to that of the real photoabsorption cross section and is rather weak, $\sim x^{-0.1}$. The second source is the variation of the $\boldsymbol{\kappa}^2$ -dependence of $f(x, \boldsymbol{\kappa})$ as x decreases. Indeed, the phenomenological studies of ref. [14] show that while the exponent $\gamma \approx 2$ is appropriate for $x_A = 0.01$, at $x_A = 0.001$ the $\boldsymbol{\kappa}^2$ -dependence of the unintegrated gluon density in the region of $\boldsymbol{\kappa}^2$ of interest corresponds to $\gamma \approx 1.7$ which lowers substantially the magnitude, and shifts to larger $\boldsymbol{\kappa}^2$ the onset of the antishadowing regime (38). Finally, because of the shift to larger \mathbf{p}^2 with decreasing x the peak value of $\Delta_{Cronin}(\mathbf{p})$ is suppressed by the $1/\mathbf{p}^2$ dependence of the antishadowing contribution, see eq. (73). This explains the numerical findings of Ref. [12].

We recall that the shown numerical results are only for the resolved interactions, any

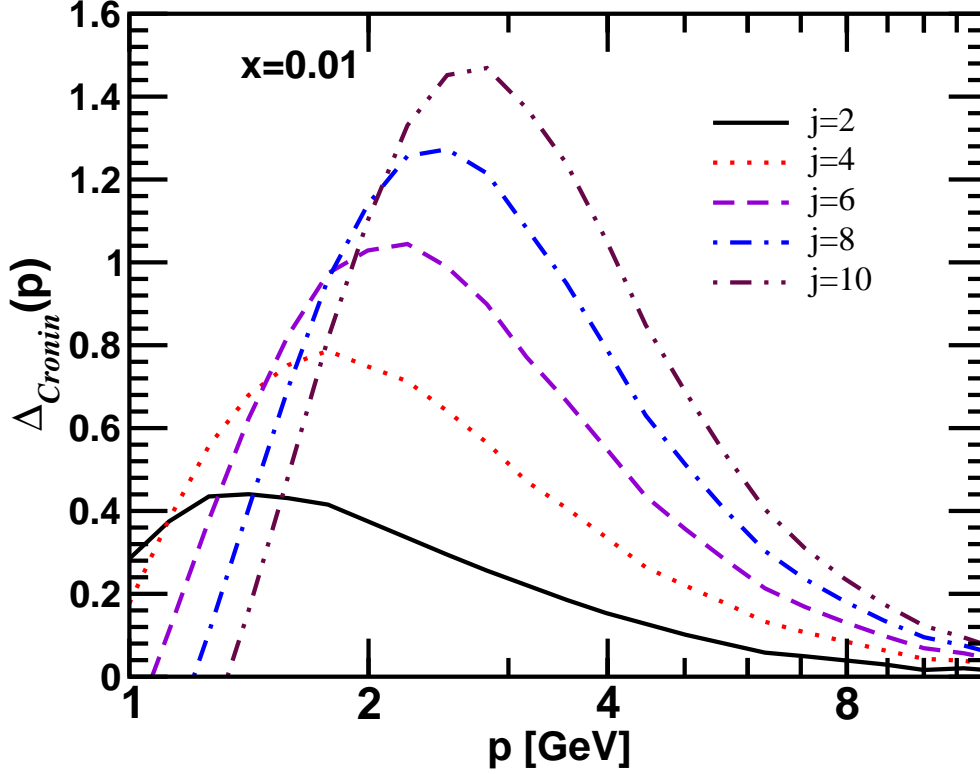


FIG. 8: (Color online) The antishadowing Cronin effect in jet production off a heavy nucleus at $x = 0.01$ as a function of the transverse momentum p of the jet parton for several multiplicities of overlapping nucleons j in the Lorentz-contracted nucleus. The production of slow quarks off nucleus with mass number $A = 200$ corresponds to $j = 4$; the production of slow gluons off nucleus with mass number $A = 200$ corresponds to $j = 8$.

comparison with the experimental data requires an application of the dilution factor (71). Also, the momentum of the observed hadrons is only a fraction of the jet momentum what places the Cronin peak for hadrons at smaller values of p than for jets.

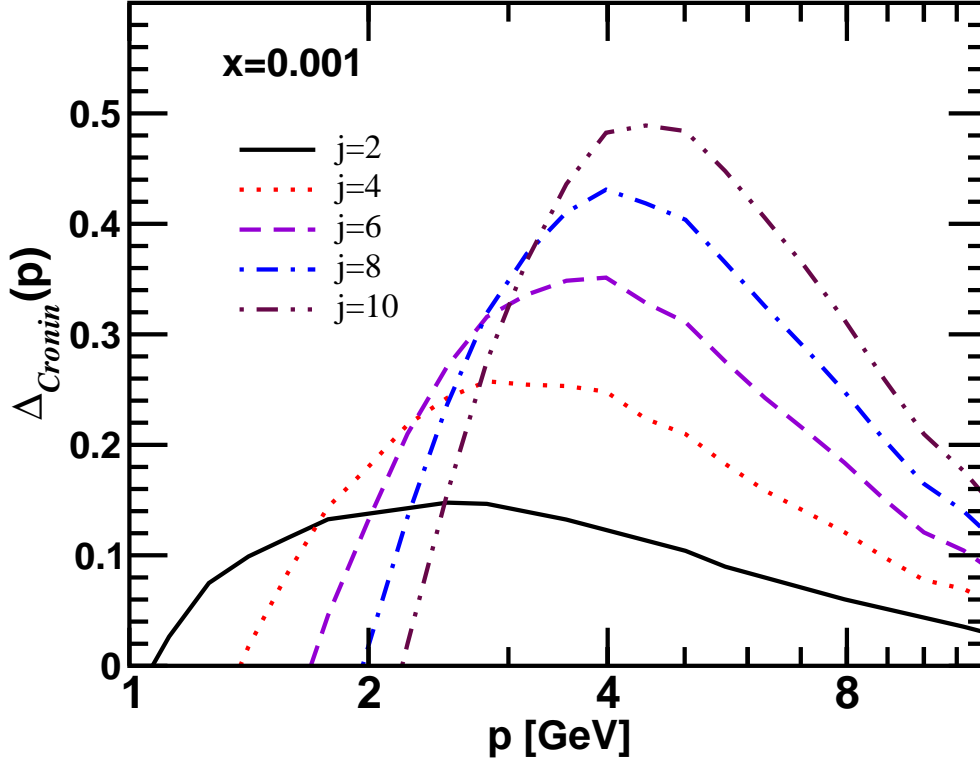


FIG. 9: (Color online) The antishadowing Cronin effect in jet production off a heavy nucleus at $x = 0.001$ as a function of the transverse momentum p of the jet parton for several multiplicities of overlapping nucleons j in the Lorentz-contracted nucleus. The production of slow quarks off nucleus with mass number $A = 200$ corresponds to $j = 4$; the production of slow gluons off nucleus with mass number $A = 200$ corresponds to $j = 8$.

VII. NONLINEAR k_{\perp} -FACTORIZATION FOR PRODUCTION OF GLUONS OFF NUCLEI

A. The gluon spectra for the free-nucleon and nuclear targets

The excitation of the gluon $g \rightarrow gg$ offers a still more remarkable example of breaking of linear k_{\perp} -factorization. In this case $a = b = c = g$ and we take the shorthand notations $z \equiv z_g$ and $\mathbf{p} \equiv \mathbf{p}_g$. The 3-parton cross section for generic three-gluon state equals

$$\sigma_{ggg}(\boldsymbol{\rho}, \mathbf{r}) = \frac{C_A}{2C_F} [\sigma_{q\bar{q}}(x, \boldsymbol{\rho}) + \sigma_{q\bar{q}}(x, \boldsymbol{\rho} - \mathbf{r}) + \sigma_{q\bar{q}}(x, \mathbf{r})] \quad (80)$$

The dipole cross section structure in eq. (16) takes the form

$$\begin{aligned} \frac{C_A}{2C_F} \{ & \sigma_{q\bar{q}}(x, \mathbf{r}) + \sigma_{q\bar{q}}(x, z\mathbf{r}') + \sigma_{q\bar{q}}(x, \mathbf{r} - z\mathbf{r}') \\ & + \sigma_{q\bar{q}}(x, \mathbf{r}') + \sigma_{q\bar{q}}(x, z\mathbf{r}) + \sigma_{q\bar{q}}(x, \mathbf{r}' - z\mathbf{r}) \\ & - 2\sigma_{q\bar{q}}(x, \mathbf{r} - \mathbf{r}') - 2\sigma_{q\bar{q}}(x, z(\mathbf{r} - \mathbf{r}')) \} \end{aligned} \quad (81)$$

Repeating the analysis of sections III and IV, for the free-nucleon case one readily finds the k_\perp -factorization representation for the gluon-jet cross section

$$\begin{aligned} \frac{d\sigma_N(g^* \rightarrow gg)}{dzd^2\mathbf{p}} &= \frac{1}{2(2\pi)^2} \int d^2\boldsymbol{\kappa} f(x_A, \boldsymbol{\kappa}) \times \frac{C_A}{2C_F} \{ |\Psi(z, \mathbf{p}) - \Psi(z, \mathbf{p} + z\boldsymbol{\kappa})|^2 \\ &+ |\Psi(z, \mathbf{p} + \boldsymbol{\kappa}) - \Psi(z, \mathbf{p} + z\boldsymbol{\kappa})|^2 + |\Psi(z, \mathbf{p}) - \Psi(z, \mathbf{p} + \boldsymbol{\kappa})|^2 \}. \end{aligned} \quad (82)$$

In agreement with the generic arguments of section IV, the abelian limit is recovered for $z \ll 1$:

$$\left. \frac{d\sigma_N(g^* \rightarrow gg)}{dzd^2\mathbf{p}} \right|_{z \ll 1} = \frac{1}{2(2\pi)^2} \int d^2\boldsymbol{\kappa} f(x_A, \boldsymbol{\kappa}) \frac{C_A}{C_F} \cdot |\Psi(z, \mathbf{p}) - \Psi(z, \mathbf{p} + \boldsymbol{\kappa})|^2. \quad (83)$$

The same abelian limit is recovered also for $z \rightarrow 1$, but this equality of two limiting cases will again be upset for nuclear targets.

Following the discussion in section VID, one can readily decompose the spectrum (83) into the contributions from the direct and resolved gluon interactions, we shall skip those details here.

The excitation of gluons into gluons, $g \rightarrow gg$, is an exceptional case for which exact formulas for a nuclear target derive without invoking the large- N_c approximation. Our result for the nuclear gluon jet spectrum reads

$$\begin{aligned} \frac{(2\pi)^2 d\sigma_A(g^* \rightarrow gg)}{dzd^2\mathbf{p}d^2\mathbf{b}} &= [S_{abs}^{(g)}(\mathbf{b})]^2 \cdot \int d^2\boldsymbol{\kappa} \phi_g(\mathbf{b}, x_A, \boldsymbol{\kappa}) \\ &\times \{ |\Psi(z, \mathbf{p}) - \Psi(z, \mathbf{p} + z\boldsymbol{\kappa})|^2 + |\Psi(z, \mathbf{p} + \boldsymbol{\kappa}) - \Psi(z, \mathbf{p} + z\boldsymbol{\kappa})|^2 + |\Psi(z, \mathbf{p}) - \Psi(z, \mathbf{p} + \boldsymbol{\kappa})|^2 \} \\ &+ S_{abs}^{(g)}(\mathbf{b}) \int d^2\boldsymbol{\kappa}_1 d^2\boldsymbol{\kappa}_2 \phi_g(\mathbf{b}, x_A, \boldsymbol{\kappa}_1) \phi_g(\mathbf{b}, x_A, \boldsymbol{\kappa}_2) \\ &\times \{ |\Psi(z, \mathbf{p} + \boldsymbol{\kappa}_1) - \Psi(z, \mathbf{p} + z\boldsymbol{\kappa}_2)|^2 + |\Psi(z, \mathbf{p} + \boldsymbol{\kappa}_1 + \boldsymbol{\kappa}_2) - \Psi(z, \mathbf{p} + z\boldsymbol{\kappa}_2)|^2 \\ &+ |\Psi(z, \mathbf{p} + \boldsymbol{\kappa}_1) - \Psi(z, \mathbf{p} + z(\boldsymbol{\kappa}_1 + \boldsymbol{\kappa}_2))|^2 \} \\ &+ \int d^2\boldsymbol{\kappa}_1 d^2\boldsymbol{\kappa}_2 d^2\boldsymbol{\kappa}_3 \phi_g(\mathbf{b}, x_A, \boldsymbol{\kappa}_1) \phi_g(\mathbf{b}, x_A, \boldsymbol{\kappa}_2) \phi_g(\mathbf{b}, x_A, \boldsymbol{\kappa}_3) \\ &\times |\Psi(z, \mathbf{p} + \boldsymbol{\kappa}_1 + \boldsymbol{\kappa}_3) - \Psi(z, \mathbf{p} + z(\boldsymbol{\kappa}_2 + \boldsymbol{\kappa}_3))|^2. \end{aligned} \quad (84)$$

Here $\phi_g(\mathbf{b}, x_A, \boldsymbol{\kappa})$ is the collective nuclear glue which now must be evaluated from

$$\begin{aligned} \Gamma_A[\mathbf{b}, \frac{C_A}{2C_F}\sigma_{q\bar{q}}(x_A, \mathbf{r})] &\equiv \int d^2\boldsymbol{\kappa}\phi_g(\mathbf{b}, x_A, \boldsymbol{\kappa})[1 - \exp[i\boldsymbol{\kappa}\mathbf{r}]], \\ S_{abs}^{(g)}(\mathbf{b}) &= \exp[-\frac{1}{2} \cdot \frac{C_A}{2C_F} \cdot \sigma_0(x_A)T(\mathbf{b})]. \end{aligned} \quad (85)$$

in which the nonabelian factor $C_A/2C_F$ enters manifestly. The emergence of a new collective gluon density $\phi_g(\mathbf{b}, x_A, \boldsymbol{\kappa}) \neq \phi(\mathbf{b}, x_A, \boldsymbol{\kappa})$ illustrates nicely the point made in [2] that the collective nuclear glue must be described by a density matrix in color space rather than by a universal scalar function. Correspondingly, the nuclear pomeron \mathbf{IP}_A^g associated with $\phi_g(\mathbf{b}, x_A, \boldsymbol{\kappa})$ is different from \mathbf{IP}_A defined for charm production off nuclei in Sect. V. The saturation scale for the gluon density $\phi_g(\mathbf{b}, x_A, \boldsymbol{\kappa})$ differs from $Q_A^2(\mathbf{b}, x_A)$ by the factor $C_A/2C_F$. Also, for hard gluons

$$f_A^{(g)}(\mathbf{b}, x_A, \boldsymbol{\kappa}) = f(x_A, \boldsymbol{\kappa}) \cdot \frac{C_A}{2C_F} \cdot \left[1 + \frac{C_A}{2C_F} \Delta_{HT}(\mathbf{b}, x_A, \boldsymbol{\kappa}) \right], \quad (86)$$

In close similarity to open charm production, the first term in eq.(84) which satisfies linear k_\perp -factorization (82) subject to the substitution of the free-nucleon $f(x_A, \boldsymbol{\kappa})$ by the collective nuclear glue $\phi_g(\mathbf{b}, x_A, \boldsymbol{\kappa})$, is suppressed by the square of the nuclear absorption factor, $[S_{abs}^{(g)}(\mathbf{b})]^2$. The second term, which is quadratic in the nuclear gluon density $\phi_g(\mathbf{b}, x_A, \boldsymbol{\kappa})$, is suppressed by $S_{abs}^{(g)}(\mathbf{b})$. What survives for strongly absorbing nuclei is the third term which is a cubic functional of collective nuclear glue $\phi_g(\mathbf{b}, x_A, \boldsymbol{\kappa})$ and the pattern of k_\perp -factorization for single gluon jet production changes from the conventional linear one for peripheral impact parameters to the cubic one for small impact parameters. The three components of the gluon spectrum can be associated with the three Kancheli-Muller diagrams of Fig. 7. A comparison of (82) and (84) shows that the nuclear cross section cannot be represented as an expansion in multiple convolutions of the free nucleon cross section as was suggested in [28]. The z -dependence of the integrands of the quadratic and cubic terms is manifestly different from that of the free-nucleon cross section. The difference between the the free-nucleon and nuclear gluon densities entails different z -distributions for free-nucleon and nuclear targets even in the linear

term. Consequently, all the three components of the nuclear spectrum will exhibit the \mathbf{p} -dependent LPM effect.

The cubic nonlinearity in terms of the collective gluon density is a pertinent feature of the radiation of gluons with finite z . Some interesting simplifications are found in the limiting case of $z \ll 1$. In this case in the quadratic and cubic terms one will encounter the quantities of the form

$$\begin{aligned} & \int d^2\boldsymbol{\kappa}_1 d^2\boldsymbol{\kappa}_2 \phi_g(\mathbf{b}, x_A, \boldsymbol{\kappa}_1) \phi_g(\mathbf{b}, x_A, \boldsymbol{\kappa}_2) |\Psi(z, \mathbf{p} + \boldsymbol{\kappa}_1 + \boldsymbol{\kappa}_2) - \Psi(z, \mathbf{p})|^2 \\ &= \int d^2\boldsymbol{\kappa} \phi_g^{(2)}(\mathbf{b}, x_A, \boldsymbol{\kappa}) |\Psi(z, \mathbf{p} + \boldsymbol{\kappa}) - \Psi(z, \mathbf{p})|^2. \end{aligned} \quad (87)$$

In terms of the convolution $\phi_g^{(2)}(\mathbf{b}, x_A, \boldsymbol{\kappa})$ the resulting single jet spectrum can be cast in the form

$$\begin{aligned} & \left. \frac{(2\pi)^2 d\sigma_A(g^* \rightarrow gg)}{dz d^2\mathbf{p} d^2\mathbf{b}} \right|_{z \ll 1} = \\ & \int d^2\boldsymbol{\kappa} \left[2S_{abs}^{(g)}(\mathbf{b}) \phi_g(\mathbf{b}, x_A, \boldsymbol{\kappa}) + \phi_g^{(2)}(\mathbf{b}, x_A, \boldsymbol{\kappa}) \right] \cdot |\Psi(z, \mathbf{p} + \boldsymbol{\kappa}) - \Psi(z, \mathbf{p})|^2, \end{aligned} \quad (88)$$

and the triple- \mathbf{IP}_A^g exchange Kancheli-Mueller diagram of Fig. 7c simplifies to the double- \mathbf{IP}_A^g exchange diagram of Fig. 7b. Finally, we observe that

$$\phi_{gg}(\mathbf{b}, x_A, \boldsymbol{\kappa}) = 2S_{abs}^{(g)}(\mathbf{b}) \phi_g(\mathbf{b}, x_A, \boldsymbol{\kappa}) + \phi_g^{(2)}(\mathbf{b}, x_A, \boldsymbol{\kappa}) \quad (89)$$

is precisely still another collective nuclear gluon density defined in terms of the gluon-gluon dipole cross section:

$$\Gamma_A[\mathbf{b}, \frac{C_A}{C_F} \sigma_{q\bar{q}}(x, \mathbf{r})] \equiv \int d^2\boldsymbol{\kappa} \phi_{gg}(\mathbf{b}, x, \boldsymbol{\kappa}) [1 - \exp[i\boldsymbol{\kappa}\mathbf{r}]] \quad (90)$$

To this end, eq. (88) is analogous to the linear k_\perp -factorization for the free nucleon case, see (83), but the free nucleon glue $f(x_A, \boldsymbol{\kappa})$ is substituted by $\phi_{gg}(\mathbf{b}, x_A, \boldsymbol{\kappa})$, which is still a nonlinear –quadratic– functional of the collective nuclear glue $\phi_g(\mathbf{b}, x_A, \boldsymbol{\kappa})$, and with which one must associate still another nuclear pomeron \mathbf{IP}_A^{gg} . In terms of $\phi_{gg}(\mathbf{b}, x_A, \boldsymbol{\kappa})$ the transverse momentum spectrum of gluon jets with $z \ll 1$ satisfies the linear k_\perp -factorization and is described by the Kancheli-Mueller diagram of Fig. 7a with $\mathbf{IP} \rightarrow \mathbf{IP}_A^{gg}$. Our final result for $z \ll 1$ coincides in its color dipole form with the one cited in [20], see also a discussion in [2], all the results for finite z are new.

B. The Cronin effect for gluons

The implications of (90) for the Cronin effect for gluon-jets are straightforward. The principal change is that for soft gluons the collective nuclear gluon density $\phi_{gg}(\mathbf{b}, x_A, \boldsymbol{\kappa})$ is obtained from $\phi(\mathbf{b}, x_A, \boldsymbol{\kappa})$ by the substitution

$$Q_A^2(\mathbf{b}, x_A) \implies Q_{A,gg}^2(\mathbf{b}, x_A) \approx \frac{C_A}{C_F} Q_A^2(\mathbf{b}, x_A), \quad (91)$$

so that the plateau in $\phi_{gg}(\mathbf{b}, x_A, \boldsymbol{\kappa})$ will be broader than in $\phi(\mathbf{b}, x_A, \boldsymbol{\kappa})$ by the factor C_A/C_F . For hard gluons

$$f_A^{(gg)}(\mathbf{b}, x_A, \boldsymbol{\kappa}) = f(x_A, \boldsymbol{\kappa}) \cdot \frac{C_A}{C_F} \cdot \left[1 + \frac{C_A}{C_F} \Delta_{HT}(\mathbf{b}, x_A, \boldsymbol{\kappa}^2) \right], \quad (92)$$

Nuclear shadowing for $\mathbf{p}^2 \lesssim Q_{A,gg}^2(\mathbf{b}, x_A)$ will be stronger than for the quark jets:

$$R_{A/N}^g(z; x_A, \mathbf{p}) = \frac{\sigma_A \left[\frac{C_A}{C_F} \sigma_0(x_A) \right]}{A \sigma_0(x_A)} \sim \frac{C_F}{C_A} R_{A/N}^Q(z; x_A, \mathbf{p}) \quad (93)$$

Evidently the antishadowing effect $\Delta_{gg}(z; x_A, \mathbf{p}) > 0$ at $\mathbf{p}^2 \gtrsim Q_{A,gg}^2(\mathbf{b}, x_A)$ will persist for gluon-jets too. Following the analysis of section VID, one would readily find that the nuclear antishadowing effect will be dominated by the resolved gluon interactions, and

$$\Delta_{gg}(z; x_A, \mathbf{p}) \approx \frac{C_A}{C_F} \Delta_{Qg}(z; x_A, \mathbf{p}). \quad (94)$$

In view of the larger saturation scale (91) the position of the peak value of the antishadowing effect for gluon jets, $\Delta_{gg}(z; x_A, \mathbf{p})$, will be placed at higher \mathbf{p}^2 than that for quark jets. For semiquantitative estimates we again invoke the numerical results for $\Delta_{Cronin}(x_A, \mathbf{p})$ shown in Fig. 4 of Ref. [12]. For heavy nuclei like gold or platinum $\langle j \rangle_g \approx \frac{C_A}{C_F} \langle j \rangle \approx 9$. At $x_A = 0.01$ quite a large peak value $\Delta_{gg}(z; x_A, \mathbf{p}) \approx 1.3$ will be reached at $p \approx 3$ GeV. At $x_A = 0.001$ the peak value $\Delta_{gg}(z; x_A, \mathbf{p}) \approx 0.45$ will be reached at $p \approx 5$ GeV. Evidently, the fragmentation of jets will shift the peak position for observed hadrons to lower values of \mathbf{p} . The antishadowing properties of the spectrum of leading gluons with $z \rightarrow 1$ are readily derived following the discussion of quark jets in section VID. The full treatment of virtual corrections to the production of leading

gluons from the lower order pQCD processes is beyond the scope of the present communication, here we only notice that they are arguably small if the transverse momentum \mathbf{p} of the observed leading gluon is much larger than the transverse momentum of the beam-gluon g^* . The leading gluon version of eq. (84) demonstrates how the pertinent nonlinearity at $z \rightarrow 1$ changes the antishadowing Cronin effect compared to the above discussed case of $z \ll 1$. Define first the two special nuclear spectra

$$\frac{(2\pi)^2 d\sigma_A^{(g^1)}}{dzd^2\mathbf{p}d^2\mathbf{b}} = \int d^2\boldsymbol{\kappa} \phi_g(\mathbf{b}, x_A, \boldsymbol{\kappa}) |\Psi(z, \mathbf{p}) - \Psi(z, \mathbf{p} + \boldsymbol{\kappa})|^2 \quad (95)$$

$$\frac{(2\pi)^2 d\sigma_A^{(g^2)}}{dzd^2\mathbf{p}d^2\mathbf{b}} = \int d^2\boldsymbol{\kappa}_1 d^2\boldsymbol{\kappa}_2 \phi_g(\mathbf{b}, x_A, \boldsymbol{\kappa}_1) \phi_g(\mathbf{b}, x_A, \boldsymbol{\kappa}_2) |\Psi(z, \mathbf{p} + \boldsymbol{\kappa}_1) - \Psi(z, \mathbf{p} + \boldsymbol{\kappa}_2)|^2, \quad (96)$$

in terms of which

$$\left. \frac{d\sigma_A(g^* \rightarrow gg)}{dzd^2\mathbf{p}d^2\mathbf{b}} \right|_{z \rightarrow 1} = 2S_{abs}^2(\mathbf{b}) \frac{d\sigma_A^{(1)}(g^* \rightarrow gg)}{dzd^2\mathbf{p}d^2\mathbf{b}} + 2S_{abs}(\mathbf{b}) \frac{(d\sigma_A^{(g^1)} \otimes \phi_g)(\mathbf{p})}{dzd^2\mathbf{p}d^2\mathbf{b}} + \frac{(d\sigma_A^{(g^2)} \otimes \phi_g)(\mathbf{p})}{dzd^2\mathbf{p}d^2\mathbf{b}}. \quad (97)$$

The small and large- \mathbf{p} properties of the first two terms in (97) have already been studied in section VI. After averaging over the azimuthal angles of $\boldsymbol{\kappa}_{1,2}$:

$$\begin{aligned} & \left\langle \left\langle |\Psi(z, \mathbf{p} + \boldsymbol{\kappa}_1) - \Psi(z, \mathbf{p} + \boldsymbol{\kappa}_2)|^2 \right\rangle \right\rangle = \\ & = \left\langle \frac{1}{(\mathbf{p} + \boldsymbol{\kappa}_1)^2} \right\rangle + \left\langle \frac{1}{(\mathbf{p} + \boldsymbol{\kappa}_2)^2} \right\rangle - \frac{2}{\mathbf{p}^2} \theta(\mathbf{p}^2 - \boldsymbol{\kappa}_1^2) \theta(\mathbf{p}^2 - \boldsymbol{\kappa}_2^2) \\ & \implies \frac{2}{|\mathbf{p}^2 - \boldsymbol{\kappa}_1^2| + \delta^2} - \frac{2}{\mathbf{p}^2} \theta(\mathbf{p}^2 - \boldsymbol{\kappa}_1^2) \theta(\mathbf{p}^2 - \boldsymbol{\kappa}_2^2), \end{aligned} \quad (98)$$

where we made a provision for the $\boldsymbol{\kappa}_1 \leftrightarrow \boldsymbol{\kappa}_2$ symmetry of the integrand. At small \mathbf{p} the last term in (98) can safely be neglected and the small- \mathbf{p} behaviour of $d\sigma^{(g^2)}$ will be similar to that of the spectrum of leading quarks (52) subject to swapping the $g \rightarrow Q\bar{Q}$ splitting function for the $g \rightarrow gg$ one as described in Appendix B. For the derivation of large- \mathbf{p} behaviour a more convenient representation is

$$\begin{aligned} \left\langle \left\langle |\Psi(z, \mathbf{p} + \boldsymbol{\kappa}_1) - \Psi(z, \mathbf{p} + \boldsymbol{\kappa}_2)|^2 \right\rangle \right\rangle & = \frac{2\boldsymbol{\kappa}_1^2}{(\mathbf{p}^2)^2} \theta(\mathbf{p}^2 - \boldsymbol{\kappa}_1^2) + \frac{2}{\boldsymbol{\kappa}_1^2} \theta(\boldsymbol{\kappa}_1^2 - \mathbf{p}^2) \\ & + \tilde{K}(\mathbf{p}^2, \boldsymbol{\kappa}_1^2) + \frac{2}{\mathbf{p}^2} \theta(\mathbf{p}^2 - \boldsymbol{\kappa}_1^2) \theta(\boldsymbol{\kappa}_2^2 - \mathbf{p}^2) \end{aligned} \quad (99)$$

The logarithmic pole contribution is absorbed in $\tilde{K}(\mathbf{p}^2, \kappa_1^2)$ which has the same properties as $K(\mathbf{p}^2, \kappa_1^2)$ in the expansion (65). Then the discussion of nuclear shadowing/antishadowing properties of these three contributions will be entirely identical to that for the quark spectrum in section VID. Following the common wisdom the logarithm $\log(\mathbf{p}^2/\mu_G^2)$ in the resolved gluon contribution, where μ_G is the appropriate infrared cutoff for gluons, must be associated with the integrated density of gluons in the beam gluon, $G_B(z, \mathbf{p}^2)$. The new item in the expansion (99) is the last term; one can readily verify that its contribution is short of the $\log \mathbf{p}^2$ and can be neglected compared to that from $\tilde{K}(\mathbf{p}^2, \kappa_1^2)$. Then, to the leading $\log \mathbf{p}^2$ approximation,

$$\begin{aligned} \frac{d\sigma_A^{(g^2)}}{dzd^2\mathbf{p}d\mathbf{b}} &= \left. \frac{d\sigma_N(g^* \rightarrow gg)}{dzd^2\mathbf{p}} \right|_{res} \cdot T(\mathbf{b}) \cdot \frac{2C_F}{C_A} \cdot \frac{f_A^{(g)}(\mathbf{b}, x_A, \mathbf{p}^2)}{f(x_A, \mathbf{p}^2)} \\ &= \left. \frac{d\sigma_N(g^* \rightarrow gg)}{dzd^2\mathbf{p}} \right|_{res} \cdot T(\mathbf{b}) \left[1 + \frac{C_A}{2C_F} \Delta_{HT}(\mathbf{b}, x_A, \mathbf{p}) \right] \end{aligned} \quad (100)$$

The dominant contribution to (97) comes from the last, nonshadowed, term in which the spectrum (100) is convoluted with $\phi_g(\mathbf{b}, x_A, \kappa)$. The convolution effect has been derived in section VID, see eq. (69), the generalization to our case gives the extra factor

$$\rho_{A/N}^{(g)}(\mathbf{p}) = 1 + \frac{C_A}{2C_F} \Delta_{HT}(\mathbf{b}, x_A, \mathbf{p}) \quad (101)$$

and

$$\left. \frac{d\Delta\sigma_A(g^* \rightarrow gg)}{dzd^2\mathbf{p}d^2\mathbf{b}} \right|_{z \rightarrow 1} = \left. \frac{d\sigma_N(g^* \rightarrow gg)}{dzd^2\mathbf{p}} \right|_{res} \cdot T(\mathbf{b}) \cdot \frac{C_A}{C_F} \Delta_{HT}(\mathbf{b}, x_A, \mathbf{p}). \quad (102)$$

A remarkable finding is that for this component of the gluon spectrum the antishadowing Cronin effect does not change from $z \ll 1$ to $z \rightarrow 1$. One can attribute that to the observation that although the nonlinear nuclear k_\perp -factorization in the two limits is of quite distinct form, the nonlinearity in the both cases is the same - a quadratic one.

VIII. GLUON RADIATION OFF QUARKS AND THE SPECTRUM OF QUARKS FROM $q^* \rightarrow gq$

A. Linear \mathbf{k}_\perp -factorization for gluon radiation off free nucleons

For completeness we show here the spectrum of gluons radiated from a fast quark that propagated the nucleus, as well as the spectrum of quarks after having shaken off their radiation cloud.

Here $a = q^*(\mathbf{b})$, $b = g(\mathbf{b}_g)$, $c = q(\mathbf{b}_q)$, where we also indicated the corresponding impact parameters. The lightcone momentum fraction carried by the gluon is z_g . Because the transverse momentum distributions of produced gluons and scattered quarks are different, for the sake of clarity we done them by \mathbf{p}_g and \mathbf{p}_q , respectively.

The relevant dipole distances are:

$$\mathbf{b}_g - \mathbf{b}_q = \mathbf{r}, \mathbf{b}' - \mathbf{b}_q = z_g \mathbf{r}', \mathbf{b}_g - \mathbf{b}'_g = \mathbf{r} - \mathbf{r}', \mathbf{b} - \mathbf{b}' = z_g(\mathbf{r} - \mathbf{r}'). \quad (103)$$

Again we start from the free nucleon case. The differential cross section is written as

$$\begin{aligned} \frac{2(2\pi)^2 d\sigma_N(q^* \rightarrow g(\mathbf{p}_g)q)}{dz_g d^2\mathbf{p}_g} &= \int d^2\mathbf{r} d^2\mathbf{r}' \exp[i\mathbf{p}_g(\mathbf{r} - \mathbf{r}')] \Psi(z_g, \mathbf{r}) \Psi^*(z_g, \mathbf{r}') \\ &\times \left\{ \sigma_3(\mathbf{r}, z_g \mathbf{r}') + \sigma_3(\mathbf{r}', z_g \mathbf{r}) - \sigma_{gg}(\mathbf{r} - \mathbf{r}') - \sigma_{q\bar{q}}(z_g(\mathbf{r} - \mathbf{r}')) \right\}, \end{aligned} \quad (104)$$

and, again, now in momentum space:

$$\begin{aligned} \frac{2(2\pi)^2 d\sigma_N(q^* \rightarrow g(\mathbf{p}_g)q)}{dz_g d^2\mathbf{p}_g} &= \\ &\int d^2\boldsymbol{\kappa} f(x_A, \boldsymbol{\kappa}) \left\{ \frac{C_A}{2C_F} \left[|\Psi(z_g, \mathbf{p}_g) - \Psi(z_g, \mathbf{p}_g + \boldsymbol{\kappa})|^2 + |\Psi(z_g, \mathbf{p}_g + \boldsymbol{\kappa}) - \Psi(z_g, \mathbf{p}_g + z_g \boldsymbol{\kappa})|^2 \right. \right. \\ &\left. \left. - |\Psi(z_g, \mathbf{p}_g) - \Psi(z_g, \mathbf{p}_g + z_g \boldsymbol{\kappa})|^2 \right] + |\Psi(z_g, \mathbf{p}_g) - \Psi(z_g, \mathbf{p}_g + z_g \boldsymbol{\kappa})|^2 \right\}. \end{aligned} \quad (105)$$

Which of course is nothing else but the QCD-'Bethe-Heitler'-Bremsstrahlung-spectrum [8] albeit in a not so familiar representation in terms of lightcone wavefunctions.

B. Nuclear case: nonlinear k_\perp factorization for gluon radiation

We quote our result in the momentum space form:

$$\begin{aligned} \frac{(2\pi)^2 d\sigma_A(q^* \rightarrow g(\mathbf{p}_g)q)}{dz_g d^2\mathbf{p}_g d^2\mathbf{b}} = \\ S_{abs}(\mathbf{b}) \int d^2\boldsymbol{\kappa} \phi(\mathbf{b}, x_A, \boldsymbol{\kappa}) \left\{ |\Psi(z_g, \mathbf{p}_g) - \Psi(z_g, \mathbf{p}_g + \boldsymbol{\kappa})|^2 + |\Psi(z_g, \mathbf{p}_g + \boldsymbol{\kappa}) - \Psi(z_g, \mathbf{p}_g + z_g \boldsymbol{\kappa})|^2 \right\} \\ + \int d^2\boldsymbol{\kappa}_1 d^2\boldsymbol{\kappa}_2 \phi(\mathbf{b}, x_A, \boldsymbol{\kappa}_1) \phi(\mathbf{b}, x_A, \boldsymbol{\kappa}_2) |\Psi(z_g, \mathbf{p}_g + z_g \boldsymbol{\kappa}_1) - \Psi(z_g, \mathbf{p}_g + \boldsymbol{\kappa}_1 + \boldsymbol{\kappa}_2)|^2. \end{aligned} \quad (106)$$

Note the by now familiar decomposition into the absorbed linear and nonlinear - quadratic - terms.

Evidently, the spectrum of soft gluons does not depend on the spin of the beam parton. Indeed, for soft gluons, $z_g \ll 1$, the result (106) simplifies to

$$\begin{aligned} \left. \frac{(2\pi)^2 d\sigma_A(q^* \rightarrow g(\mathbf{p}_g)q)}{dz_g d^2\mathbf{p}_g d^2\mathbf{b}} \right|_{z_g \ll 1} = \\ \int d^2\boldsymbol{\kappa} \left\{ 2S_{abs}(\mathbf{b}) \phi(\mathbf{b}, x_A, \boldsymbol{\kappa}) + \phi^{(2)}(\mathbf{b}, x_A, \boldsymbol{\kappa}) \right\} |\Psi(z_g, \mathbf{p}_g) - \Psi(z_g, \mathbf{p}_g + \boldsymbol{\kappa})|^2 \\ = \int d^2\boldsymbol{\kappa} \phi_{gg}(\mathbf{b}, x_A, \boldsymbol{\kappa}) |\Psi(z_g, \mathbf{p}_g) - \Psi(z_g, \mathbf{p}_g + \boldsymbol{\kappa})|^2, \end{aligned} \quad (107)$$

which is a precise counterpart of eq. (88) for the $g^* \rightarrow gg$ breakup. In the large- N_c approximation $\phi_g(\mathbf{b}, x_A, \boldsymbol{\kappa}) = \phi(\mathbf{b}, x_A, \boldsymbol{\kappa})$ and $(\phi \otimes \phi)(\mathbf{b}, x_A, \boldsymbol{\kappa}) = \phi_{gg}(\mathbf{b}, x_A, \boldsymbol{\kappa})$.

Consequently, the antishadowing Cronin effect for slow gluons from $q^* \rightarrow qg$ will be identical to that from $g^* \rightarrow gg$,

$$\Delta_{gq}(z_g \ll 1; x_A, \mathbf{p}_g) = \Delta_{gg}(z_g \ll 1; x_A, \mathbf{p}_g) = 2\Delta_{Qg}(z_Q \ll 1; x_A, \mathbf{p}_g). \quad (108)$$

For the numerical estimates for pAu collisions one must take $\Delta_{Cronin}(x_A, \mathbf{p}_g)$ for $j = 8$ in Figs. 8, 9. On the other hand a comparison of eqs. (106) and (31) shows that the spectrum of leading gluons with $z_g \rightarrow 1$ from $q^* \rightarrow qg$ will have precisely the same convolution form (35) as the spectrum of leading quarks from $g^* \rightarrow Q\bar{Q}$ which in view of the findings of sections VID and VII B entails

$$\Delta_{gq}(z_g \rightarrow 1; x_A, \mathbf{p}_g) = \Delta_{Qg}(z_Q \rightarrow 1; x_A, \mathbf{p}_g) = \Delta_{gg}(z_g \rightarrow 1; x_A, \mathbf{p}_g). \quad (109)$$

This finding suggests that the equality of antishadowing Cronin effect for leading and soft gluons does not depend on the beam parton be it a quark or a gluon.

C. \mathbf{p}_q -spectrum of quarks from the breakup $q^* \rightarrow gq$ on a free nucleon

We now turn to our last application, the spectrum of quarks from the excitation of the qg -Fock state of a fast quark. In the practically interesting case of forward quark jets in pA collisions at RHIC the beam quarks q^* have small transverse momentum and the production of high- \mathbf{p} quarks is not affected by virtual radiative corrections, see the discussion in Sect. VII B. Without further details we quote again first the dipole representation:

$$\frac{2(2\pi)^2 d\sigma_N(q^* \rightarrow q(\mathbf{p}_q)g)}{dz_q d^2\mathbf{p}_q} = \int d^2\mathbf{r} d^2\mathbf{r}' \Psi(z_q, \mathbf{r}) \Psi^*(z_q, \mathbf{r}') \exp[i\mathbf{p}_q(\mathbf{r} - \mathbf{r}')] \{ \sigma_3(\mathbf{r}, \mathbf{r} - z_q \mathbf{r}') + \sigma_3(\mathbf{r}', \mathbf{r}' - z_q \mathbf{r}) - \sigma_{q\bar{q}}(\mathbf{r} - \mathbf{r}') - \sigma_{q\bar{q}}(z_q(\mathbf{r} - \mathbf{r}')) \}, \quad (110)$$

while the linear k_\perp -factorization result reads

$$\frac{2(2\pi)^2 d\sigma_N(q^* \rightarrow q(\mathbf{p}_q)g)}{dz_q d^2\mathbf{p}_q} = \int d^2\boldsymbol{\kappa} f(x_A, \boldsymbol{\kappa}) \left\{ \frac{C_A}{2C_F} \left[|\Psi(z_q, \mathbf{p}_q) - \Psi(z_q, \mathbf{p}_q + \boldsymbol{\kappa})|^2 + |\Psi(z_q, \mathbf{p}_q) - \Psi(z_q, \mathbf{p}_q + z_q \boldsymbol{\kappa})|^2 - |\Psi(z_q, \mathbf{p}_q + \boldsymbol{\kappa}) - \Psi(z_q, \mathbf{p}_q + z_q \boldsymbol{\kappa})|^2 \right] + |\Psi(z_q, \mathbf{p}_q + \boldsymbol{\kappa}) - \Psi(z_q, \mathbf{p}_q + z_q \boldsymbol{\kappa})|^2 \right\}. \quad (111)$$

A closer comparison of the \mathbf{p} spectra of gluons and quarks from $g^* \rightarrow gq$ reveals interesting differences which hold in both the nonabelian and abelian, $C_A \rightarrow 0$, cases. Evidently, in the \mathbf{p} -integrated spectra we would obtain the longitudinal spectrum of quarks simply by swapping $z_g \rightarrow 1 - z_g = z_q$ in the formula for the gluon spectrum and vice versa. The similar procedure for the \mathbf{p} -spectra, as advocated in [21] would be entirely wrong.

D. Quark spectrum from the breakup of the qg -Fock state of a fast quark on a nuclear target

Routine application of the above described technique yields

$$\frac{(2\pi)^2 d\sigma_A(q^* \rightarrow q(\mathbf{p}_q)g)}{dz_q d^2\mathbf{p}_q d^2\mathbf{b}} =$$

$$S_{abs}(\mathbf{b}) \int d^2\boldsymbol{\kappa} \phi(\mathbf{b}, x_A, \boldsymbol{\kappa}) \left\{ |\Psi(z_q, \mathbf{p}_q) - \Psi(z_q, \mathbf{p}_q + \boldsymbol{\kappa})|^2 + |\Psi(z_q, \mathbf{p}_q) - \Psi(z_q, \mathbf{p}_q + z_q \boldsymbol{\kappa})|^2 \right\} \\ + \int d^2\boldsymbol{\kappa}_1 d^2\boldsymbol{\kappa}_2 \phi(\mathbf{b}, x_A, \boldsymbol{\kappa}_1) \phi(\mathbf{b}, x_A, \boldsymbol{\kappa}_2) |\Psi(z_q, \mathbf{p}_q + \boldsymbol{\kappa}_1) - \Psi(z_q, \mathbf{p}_q + z_q \boldsymbol{\kappa}_2)|^2. \quad (112)$$

As usual, the absorbed linear k_\perp -factorization term is the counterpart of the large- N_c free-nucleon spectrum (111). Note also that the \mathbf{p}_q -spectrum of slow quark jets from $q^* \rightarrow qg$ coincides with the spectrum (34) from $g^* \rightarrow Q\bar{Q}$ and the Cronin effect for the two cases will be identical:

$$\Delta_{qq}(z_q \ll 1; x_A, \mathbf{p}_q) = \Delta_{Qg}(z_Q \ll 1; x_A, \mathbf{p}_q). \quad (113)$$

For the numerical estimates for pAu collisions one must take $\Delta_{Cronin}(x_A, \mathbf{p}_q)$ for $j = 4$ in Figs. 8, 9.

The spectrum of leading-quark jets, $z_q \rightarrow 1$, equals

$$\frac{(2\pi)^2 d\sigma_A(q^* \rightarrow q(\mathbf{p}_q)g)}{dz_q d^2\mathbf{p}_q d^2\mathbf{b}} \Big|_{z_q \rightarrow 1} = 2 S_{abs}(\mathbf{b}) \int d^2\boldsymbol{\kappa} \phi(\mathbf{b}, x_A, \boldsymbol{\kappa}) |\Psi(z_q, \mathbf{p}_q) - \Psi(z_q, \mathbf{p}_q + \boldsymbol{\kappa})|^2 \\ + \int d^2\boldsymbol{\kappa}_1 d^2\boldsymbol{\kappa}_2 \phi(\mathbf{b}, x_A, \boldsymbol{\kappa}_1) \phi(\mathbf{b}, x_A, \boldsymbol{\kappa}_2) |\Psi(z_q, \mathbf{p}_q + \boldsymbol{\kappa}_1) - \Psi(z_q, \mathbf{p}_q + \boldsymbol{\kappa}_2)|^2, \quad (114)$$

where the second term is similar to $d\sigma^{(2g)}$ of eq. (96) which emerged in the discussion of the spectrum of leading gluons from $g^* \rightarrow gg$. Its antishadowing properties have been studied in section VII B and entail

$$\Delta_{qq}(z_q \rightarrow 1; x_A, \mathbf{p}_q) = \Delta_{qq}(z_q \ll 1; x_A, \mathbf{p}_q) \quad (115)$$

The antishadowing effect for leading quarks from $q \rightarrow qg$ is one half of that for leading gluons from $g \rightarrow gg$.

The above derived z_q -distribution quantifies the energy loss for the radiation of gluons, i.e., gives a solution of the LPM problem for finite transverse momentum \mathbf{p} of the observed quark jet. The case of quark jets is important for its relevance to the large pseudorapidity, high- \mathbf{p} hadron production in deuteron-gold collisions at RHIC. The numerical studies of the LPM effect contribution to nuclear quenching of forward high- \mathbf{p} hadrons observed experimentally by the BRAHMS collaboration [18] will be reported elsewhere.

IX. DISCUSSION OF THE RESULTS

Extending the technique developed earlier [2] we elucidated the pattern of k_{\perp} -factorization breaking for the single gluon and quark jet production from $g^* \rightarrow Q\bar{Q}$, $g^* \rightarrow gg$, $q^* \rightarrow qg$ breakup on nuclear targets. In all the cases we derived an explicit nonlinear, from quadratic to cubic, k_{\perp} -factorization representations for the inclusive single-jet transverse and longitudinal momentum spectra in terms of the collective nuclear unintegrated gluon density. The results are simple and elegant and have not been presented in this form in the existing literature on the subject. They also give a solution of the LPM problem for finite transverse momentum \mathbf{p} of the observed secondary quark and gluon jet. One of the evident future applications will be to the nuclear quenching of forward high- \mathbf{p} hadrons observed experimentally by the BRAHMS collaboration [18].

The unintegrated collective nuclear gluon density which defines the nuclear observables is shown to change from the quark to gluon observables even within the same process what exemplifies the point that an ultrarelativistic nucleus can not be described by a single gluon density, the collective nuclear density must rather be described by a density matrix in color space [2]. The often used linear k_{\perp} -factorization description of particle production off nuclei (e.g. [23], for the recent applications and more references see also [24, 25, 29, 30]) is definitely not borne out by the multiple scattering theory. There is a striking contrast to the single-quark jet transverse momentum spectrum from $\gamma^* \rightarrow q\bar{q}$ breakup on a nucleus for which linear k_{\perp} -factorization is fulfilled, and our analysis shows that that the linear k_{\perp} -factorization in $\gamma^* \rightarrow q\bar{q}$ is rather an exception due to the color-singlet nature of the photon by which the single-jet spectrum accidentally becomes an abelian problem [2].

Although the linear k_{\perp} -factorization for hard processes in nuclei does not exist, for all breakup processes we identified the ‘abelian’ regime in which the transverse momentum spectra of soft quark and gluons jets with $z_{q,g} \ll 1$ take the process-dependent linear k_{\perp} -factorization form. Specifically, the production of quark jets is described by the collective gluon density $\phi(\mathbf{b}, x_A, \boldsymbol{\kappa})$ defined for the triplet-antitriplet color dipole. The production

of gluon jets is described in terms of the collective gluon density $\phi_{gg}(\mathbf{b}, x_A, \boldsymbol{\kappa})$ defined for the octet-octet color dipole. The color-dipole representation for such a slow gluon limit coincides with that derived before for the slow gluon production by Kovchegov and Mueller [20]. The reason behind the recovery of the Kovchegov-Mueller form for slow jets is that in this limit the single-parton spectrum becomes an abelian problem [2]. Such a form is of limited practical significance, though. Evidently, the limit of $z_q \ll 1$ is irrelevant to the open charm production, in the gluon jet production too the dominant contribution to the observed jet cross section will come from finite z to be described by our nonlinear k_\perp -factorization. The full z -dependence is also mandatory for the evaluation of the LPM quenching of forward high- \mathbf{p} jets. The production of gluons from $g \rightarrow g_1 g_2$ has been discussed also in [22], their equation for the nuclear spectrum contradicts our general result (17). The earlier work on $q \rightarrow qg$ by [21] starts with the two-parton inclusive spectrum. When compared to our general equation (17), in ref. [21] the coupled-channel S-matrix $S_{q\bar{q}gg}^{(4)}$ has illegitimately been substituted by a single-channel Glauber exponential. Despite this inconsistency, the final color dipole representation of Ref. [21] for the single-parton spectrum agrees with ours.

Recently, the production of heavy quarks from the excitation $q \rightarrow q'g$, $g \rightarrow Q\bar{Q}$ has been discussed in the color dipole framework in ref. [31]. We have however not been able to reconcile the results given there with our findings on the cancellation of spectator interactions. Very recent works [29, 32] start with the reference to the color glass condensate model, but in actual applications the Glauber-Gribov multiple scattering theory is used and a quantity similar to the collective unintegrated glue of [2, 12] is introduced. Although no explicit formulas corresponding to eq.(31) for the heavy quark cross section are given, the authors are aware in part of our criticism [2] of the applicability of linear k_\perp factorization in the saturation regime.

Regarding the applicability domain of our formalism the considered processes correspond to production of parton pairs with $x_{b,c} \lesssim x_A \sim 10^{-2}$, where $x_{b,c}$ are defined with respect to the nucleus. In the pA collisions at RHIC this requires that both partons were produced in the proton hemisphere. The consistent discussion of higher order processes

and of the emerging BFKL evolution of nuclear spectra remains an open problem. Generally speaking one will have to address a situation in which the coherence of more than two partons over the nucleus is important, and the question is in how far the rescattering of partons faster/slower than the measured jet is reabsorbed into the (non-)linear evolution of the beam/target effective gluon densities. Such evolution effects would perhaps not feature too prominently at RHIC energies, where the rapidity span overlaps well with the applicability region of our approach. Still such studies will be important to establish the viability of our approach to higher energies such as LHC. They would also sharpen our understanding of the similarities and differences of our color dipole formalism and the Color Glass Condensate approach (for recent explorations of the energy dependence of the Cronin effect for slow gluon production within those models, see e.g. [24–27, 32–34]).

The most obvious application of the derived nonlinear nuclear k_{\perp} -factorization is to nuclear effects in the single-jet spectrum which are usually referred to as the Cronin effect. Our derivation unambiguously relates it to the antishadowing property of the collective nuclear gluon density [2, 12]. The Cronin effect was shown to exhibit interesting variations across the phase space. Based on the numerical studies of the antishadowing effect in the collective nuclear gluon density [12] we presented numerical estimates for the Cronin effect. One feature of these estimates is noteworthy: The realistic models for the unintegrated gluon density of the proton [14] suggest a somewhat small value of the saturation scale, $Q_A \approx 1$ GeV, even for the heaviest nuclei. Still, the Cronin effect is found to reach its peak value at $|\mathbf{p}| \approx (2 \div 2.5)$ GeV, which is well within the pQCD domain.

To summarize, our analysis establishes nonlinear k_{\perp} -factorization as a universal feature of hard production off nuclear targets. The presented formalism can readily be extended to the nuclear dependence of jet-jet correlations and nuclear quenching of forward quark jets, the corresponding work is in progress.

Acknowledgements: We are grateful to B.G. Zakharov for illuminating discussions and suggestions.

Appendix A: The derivation of $S^{(n)}$

Here we expose some of the technicalities behind the derivation of the master equation (10) and the reduction of the four-parton S -matrix to the two-body S -matrices in equation (14). The color-dipole properties of excitation amplitudes are elucidated and the calculation of the S -matrices $S^{(n)}$ is greatly simplified in the $q\bar{q}$ representation of the gluon interactions. We demonstrate the principal virtues of this technique on an example of $g^* \rightarrow Q\bar{Q}$ on a free-nucleon target, for the extension to a nuclear target see [2]. In the color space the $g_a Q\bar{Q}$ vertex contains the $SU(N_c)$ generator t^a , so that in the quark color space the contribution of the diagram of fig. 3b is proportional to $S(\mathbf{b}_b)t^a S^\dagger(\mathbf{b}_c)$, whereas the contribution of the diagram of fig. 3c is proportional to $-t^d S_{da}(\mathbf{b})$. Here $S^\dagger(\mathbf{b}_c)$ describes the interaction of the antiquark, and $S_{da}(\mathbf{b}) = \langle g_d | S_g(\mathbf{b}) | g_a \rangle$ describes the transition between the two gluons in color states a and d . Consequently, the properly normalized excitation operator is

$$\mathcal{M}_a(\mathbf{b}_b, \mathbf{b}_c, \mathbf{b}) = \frac{1}{\sqrt{C_F N_c}} \left(S(\mathbf{b}_b) t^a S^\dagger(\mathbf{b}_c) - t^d S_{da}(\mathbf{b}) \right) \quad (\text{A.1})$$

where $C_F N_c = \text{Tr } t^a t^a$. The above vertex operators t^a have been suppressed in the expansion (6).

Now we note that

$$S_{da}(\mathbf{b}) = \frac{1}{T_F} \text{Tr} \left(t^d S(\mathbf{b}) t^a S^\dagger(\mathbf{b}) \right) \quad (\text{A.2})$$

and, upon the Fierz transformation,

$$t^d S_{da}(\mathbf{b}) = S(\mathbf{b}) t^a S^\dagger(\mathbf{b}), \quad (\text{A.3})$$

which leads to a particularly simple form of the excitation operator:

$$\mathcal{M}_a(\mathbf{b}_b, \mathbf{b}_c, \mathbf{b}) = \frac{1}{\sqrt{C_F N_c}} \left(S(\mathbf{b}_b) t^a S^\dagger(\mathbf{b}_c) - S(\mathbf{b}) t^a S^\dagger(\mathbf{b}) \right) \quad (\text{A.4})$$

Note how $\mathcal{M}_a(\mathbf{b}_b, \mathbf{b}_c, \mathbf{b})$ vanishes if $\mathbf{b}_b = \mathbf{b}_c = \mathbf{b}$: in this limit the $Q\bar{Q}$ behaves as a pointlike color-octet state indistinguishable from the gluon and its $Q\bar{Q}$ structure can not be resolved. What enters the integrand of (10) is $\text{Tr} \left(\mathcal{M}_a^\dagger(\mathbf{b}'_b, \mathbf{b}'_c, \mathbf{b}') \mathcal{M}_a(\mathbf{b}_b, \mathbf{b}_c, \mathbf{b}) \right)$.

Before proceeding further we notice that the S -matrix for the color singlet $q\bar{q}$ dipole equals

$$S_2(\mathbf{b}_b - \mathbf{b}_c) = \frac{1}{N_c} \text{Tr} \left(S(\mathbf{b}_b) S^\dagger(\mathbf{b}_c) \right) = 1 - \Gamma_2(\mathbf{B}, \mathbf{b}_b - \mathbf{b}_c), \quad (\text{A.5})$$

where $\mathbf{r} = \mathbf{b}_b - \mathbf{b}_c$ is the relevant dipole size and $\Gamma_2(\mathbf{B}, \mathbf{b}_b - \mathbf{b}_c)$ is the corresponding profile function. Upon the integration over the dipole impact parameter, \mathbf{B} , one finds the color-dipole cross section

$$\sigma_{q\bar{q}}(x, \mathbf{r}) = 2 \int d^2 \mathbf{B} \Gamma_2(\mathbf{B}, \mathbf{r}). \quad (\text{A.6})$$

The excitation on a free nucleon target is described to the single-gluon exchange approximation. In this approximation

$$S_2^2(\mathbf{b}_b - \mathbf{b}_c) = 1 - 2\Gamma_2(\mathbf{B}, \mathbf{b}_b - \mathbf{b}_c), \quad (\text{A.7})$$

Now we can identify the $S^{(n)}$ in the integrand of (10) and give explicit expressions in terms of $\Gamma_2(\mathbf{B}, \mathbf{r})$. Making use of

$$\text{Tr} \left(t^a A t^a B \right) = \frac{1}{2} \left(\text{Tr} (A) \cdot \text{Tr} (B) - \frac{1}{N_c} \text{Tr} (AB) \right) \quad (\text{A.8})$$

and applying the unitarity condition (13) wherever appropriate one readily finds

$$S^{(2)}(\mathbf{b}, \mathbf{b}') = \frac{1}{C_F N_c} \text{Tr} \left(S(\mathbf{b}') t^a S^\dagger(\mathbf{b}') S(\mathbf{b}) t^a S^\dagger(\mathbf{b}) \right) = 1 - \frac{C_A}{C_F} \Gamma_2(\mathbf{B}, \mathbf{b}' - \mathbf{b}) \quad (\text{A.9})$$

$$S^{(3)}(\mathbf{b}_b, \mathbf{b}_c, \mathbf{b}') = \frac{1}{C_F N_c} \text{Tr} \left(S(\mathbf{b}_b) t^a S^\dagger(\mathbf{b}_c) S(\mathbf{b}') t^a S^\dagger(\mathbf{b}') \right) \quad (\text{A.10})$$

$$= 1 - \left\{ \frac{C_A}{2C_F} \left(\Gamma_2(\mathbf{B}, \mathbf{b}' - \mathbf{b}_b) + \Gamma_2(\mathbf{B}, \mathbf{b}' - \mathbf{b}_c) \right) - \frac{1}{N_c^2 - 1} \Gamma_2(\mathbf{B}, \mathbf{b}_b - \mathbf{b}_c) \right\}$$

$$S^{(3)}(\mathbf{b}'_b, \mathbf{b}'_c, \mathbf{b}) = \frac{1}{C_F N_c} \text{Tr} \left(S(\mathbf{b}'_b) t^a S^\dagger(\mathbf{b}'_c) S(\mathbf{b}) t^a S^\dagger(\mathbf{b}) \right)$$

$$= 1 - \left\{ \frac{C_A}{2C_F} \left(\Gamma_2(\mathbf{B}, \mathbf{b} - \mathbf{b}'_b) + \Gamma_2(\mathbf{B}, \mathbf{b} - \mathbf{b}'_c) \right) - \frac{1}{N_c^2 - 1} \Gamma_2(\mathbf{B}, \mathbf{b}'_b - \mathbf{b}'_c) \right\}. \quad (\text{A.11})$$

In the $S^{(3)}$ one readily identifies the profile functions of the $q\bar{q}g$ cross section as introduced in [37]. The case of $S^{(4)}$ is more tricky:

$$S^{(4)}(\mathbf{b}_b, \mathbf{b}_c, \mathbf{b}'_b, \mathbf{b}'_c) = \frac{1}{C_F N_c} \text{Tr} \left(S(\mathbf{b}_b) t^a S^\dagger(\mathbf{b}_c) S(\mathbf{b}'_c) t^a S^\dagger(\mathbf{b}'_b) \right)$$

$$\begin{aligned}
&= \frac{1}{N_c^2 - 1} \left\{ N_c^2 \left(1 - \Gamma_2(\mathbf{B}, \mathbf{b}_c - \mathbf{b}'_c) - \Gamma_2(\mathbf{B}, \mathbf{b}_b - \mathbf{b}'_b) \right) \right. \\
&\quad \left. - \frac{1}{N_c} \text{Tr} \left[S(\mathbf{b}_b) S^\dagger(\mathbf{b}_c) S(\mathbf{b}'_c) S^\dagger(\mathbf{b}'_b) \right] \right\}. \tag{A.12}
\end{aligned}$$

The last term in (A.12) is an operator in the $q\bar{q}$ color space and in general $S^{(4)}$ is the coupled-channel operator derived in [2]. In the case of the single-particle particle spectrum $\mathbf{b}'_c = \mathbf{b}_c$ and the straightforward application of the unitarity condition (13) yields

$$S^{(4)}(\mathbf{b}_b, \mathbf{b}_c, \mathbf{b}'_b, \mathbf{b}_c) = S_2(\mathbf{b}_b - \mathbf{b}'_b) = 1 - \Gamma_2(\mathbf{B}, \mathbf{b}_b - \mathbf{b}'_b). \tag{A.13}$$

As quoted above the results are for the free nucleon target, for the nuclear target one must apply the Glauber–Gribov exponentiation to the relevant $S^{(n)}$.

Appendix B:

In all the transverse momentum spectra the recurrent quantity is $|\Psi(z, \mathbf{p}) - \Psi(z, \mathbf{p} - \boldsymbol{\kappa})|^2$. This quantity for the incident photon is found in [2, 5]. For transverse photons and flavor f , i.e., for the $\gamma^* \rightarrow Q\bar{Q}$ excitation,

$$\begin{aligned}
&|\Psi(z, \mathbf{p}) - \Psi(z, \mathbf{p} - \boldsymbol{\kappa})|^2 = 2N_c e_Q^2 \alpha_{em} \\
&\times \left\{ [z^2 + (1-z)^2] \left(\frac{\mathbf{p}}{\mathbf{p}^2 + \varepsilon^2} - \frac{\mathbf{p} - \boldsymbol{\kappa}}{(\mathbf{p} - \boldsymbol{\kappa})^2 + \varepsilon^2} \right)^2 \right. \\
&\quad \left. + m_Q^2 \left(\frac{1}{\mathbf{p}^2 + \varepsilon^2} - \frac{1}{(\mathbf{p} - \boldsymbol{\kappa})^2 + \varepsilon^2} \right)^2 \right\}, \tag{B.1}
\end{aligned}$$

The term $\propto m_Q^2$ must only be kept for heavy quarks. The same quantity for the $g^* \rightarrow Q\bar{Q}$ is obtained from (B.1) by the substitution $N_c e_Q^2 \alpha_{em} \rightarrow T_F \alpha_S(Q_a^2)$ and the substitution in (B.2) of the virtuality of the photon Q^2 by the virtuality of the beam gluon $Q_{g^*}^2$. For the general case $a \rightarrow bc$

$$\varepsilon^2 = z_b z_c Q_a^2 + z_b m_c^2 + z_c m_b^2, \tag{B.2}$$

where Q_a^2 is the virtuality of parton a and the mass dependent term is important for heavy flavours. Now note that the factor $T_F[z^2 + (1-z)^2]$ which emerges in the first

term in the rhs of (B.1) is precisely the familiar splitting function $P_{Qg}(z)$. For all other cases $|\Psi(z, \mathbf{p}) - \Psi(z, \mathbf{p} - \boldsymbol{\kappa})|^2$ is obtained from that for $g^* \rightarrow Q\bar{Q}$ by the substitution of $P_{Qg}(z)$ by the real-emission part of the relevant splitting function for $z < 1$ found in all textbooks [1]. Take for instance the fragmentation of light quarks $q \rightarrow qq$. The $|\Psi(z_q, \mathbf{p}) - \Psi(z_q, \mathbf{p} - \boldsymbol{\kappa})|^2$ which enters the spectrum of quarks must be evaluated with the splitting function

$$P_{qq}(z_q) = C_F \frac{1 + z_q^2}{(1 - z_q)}. \quad (\text{B.3})$$

The $|\Psi(z_g, \mathbf{p}) - \Psi(z_g, \mathbf{p} - \boldsymbol{\kappa})|^2$ which enters the spectrum of gluons in the same process must be evaluated with

$$P_{gq}(z_g) = C_F \frac{1 + (1 - z_g)^2}{z_g}. \quad (\text{B.4})$$

In the fragmentation of gluons $g \rightarrow gg$ one must take $|\Psi(z, \mathbf{p}) - \Psi(z, \mathbf{p} - \boldsymbol{\kappa})|^2$ with the splitting function

$$P_{gg}(z) = 2C_A \left[\frac{1 - z}{z} + \frac{z}{1 - z} + z(1 - z) \right]. \quad (\text{B.5})$$

If ε^2 is negligible small compared to \mathbf{p}^2 , then one can use the large- \mathbf{p} approximation:

$$\left(\frac{\mathbf{p}}{\mathbf{p}^2} - \frac{\mathbf{p} - \boldsymbol{\kappa}}{(\mathbf{p} - \boldsymbol{\kappa})^2} \right)^2 = \frac{\boldsymbol{\kappa}^2}{\mathbf{p}^2(\mathbf{p} - \boldsymbol{\kappa})^2}, \quad (\text{B.6})$$

and it is worth to recall the emerging exact factorization of longitudinal and transverse momentum dependencies which is a well known feature of the high energy limit.

-
- [1] E. Leader and E. Predazzi, Introduction to Gauge Theories and Modern Particle Physics, vols.1 & 2, Cambridge University Press, Cambridge, 1996; G. Sterman, An Introduction to Quantum Field Theory, Cambridge University Press, Cambridge, 1993; R. K. Ellis, W. J. Stirling and B. R. Webber, "QCD and collider physics," Cambridge Monogr. Part. Phys. Nucl. Phys. Cosmol. **8**, 1 (1996).
- [2] N. N. Nikolaev, W. Schäfer, B. G. Zakharov and V. R. Zoller, J. Exp. Theor. Phys. **97**, 441 (2003) [Zh. Eksp. Teor. Fiz. **124**, 491 (2003)].

- [3] B. Andersson *et al.* [Small x Collaboration], *Eur. Phys. J. C* **25**, 77 (2002); J. R. Andersen *et al.* [Small x Collaboration], *Eur. Phys. J. C* **35**, 67 (2004)
- [4] N.N. Nikolaev and V.I. Zakharov, *Sov. J. Nucl. Phys.* **21**, 227 (1975) [*Yad. Fiz.* **21**, 434 (1975)]; *Phys. Lett. B* **55**, 397 (1975).
- [5] N. N. Nikolaev and B. G. Zakharov, *Z. Phys. C* **49**, 607 (1991).
- [6] V. Barone, M. Genovese, N. N. Nikolaev, E. Predazzi and B. G. Zakharov, *Z. Phys. C* **58**, 541 (1993).
- [7] N. N. Nikolaev, G. Piller and B. G. Zakharov, *J. Exp. Theor. Phys.* **81**, 851 (1995) [*Zh. Eksp. Teor. Fiz.* **108**, 1554 (1995)]; *Z. Phys. A* **354**, 99 (1996).
- [8] B. G. Zakharov, *JETP Lett.* **63**, 952 (1996); *JETP Lett.* **65**, 615 (1997); *Phys. Atom. Nucl.* **61**, 838 (1998) [*Yad. Fiz.* **61**, 924 (1998)].
- [9] R. Baier, D. Schiff and B. G. Zakharov, *Ann. Rev. Nucl. Part. Sci.* **50**, 37 (2000).
- [10] N. N. Nikolaev, W. Schäfer, B. G. Zakharov and V. R. Zoller, arXiv:hep-ph/0406085.
- [11] J. W. Cronin, H. J. Frisch, M. J. Shochet, J. P. Boymond, R. Mermod, P. A. Piroué and R. L. Sumner, *Phys. Rev. D* **11**, 3105 (1975).
- [12] N. N. Nikolaev, W. Schäfer and G. Schwiete, *Phys. Rev. D* **63**, 014020 (2001).
- [13] N. N. Nikolaev, W. Schäfer and G. Schwiete, *JETP Lett.* **72**, 405 (2000) [*Pisma Zh. Eksp. Teor. Fiz.* **72**, 583 (2000)].
- [14] I. P. Ivanov and N. N. Nikolaev, *Phys. Atom. Nucl.* **64**, 753 (2001) [*Yad. Fiz.* **64**, 813 (2001)]; *Phys. Rev. D* **65**, 054004 (2002).
- [15] Y. Zhang, G. I. Fai, G. Papp, G. G. Barnafoldi and P. Levai, *Phys. Rev. C* **65**, 034903 (2002); G. G. Barnafoldi, G. Papp, P. Levai and G. Fai, *J. Phys. G* **30**, S1125 (2004).
- [16] W. Cassing, K. Gallmeister and C. Greiner, *Nucl. Phys. A* **735**, 277 (2004).
- [17] R. C. Hwa and C. B. Yang, *Phys. Rev. Lett.* **93**, 082302 (2004).
- [18] I. Arsene *et al.* [BRAHMS Collaboration], arXiv:nucl-ex/0403005.
- [19] O. V. Kancheli, *JETP Lett.* **11**, 267 (1970) [*Pisma Zh. Eksp. Teor. Fiz.* **11**, 397 (1970)]; V. A. Abramovsky, O. V. Kancheli and I. D. Mandzhavidze, *Yad. Fiz.* **13**, 1102 (1971); A. H. Mueller, *Phys. Rev. D* **2**, 2963 (1970).

- [20] Y. V. Kovchegov and A. H. Mueller, Nucl. Phys. B **529**, 451 (1998); Y. V. Kovchegov and K. Tuchin, Phys. Rev. D **65**, 074026 (2002).
- [21] B. Z. Kopeliovich, A. V. Tarasov and A. Schäfer, Phys. Rev. C **59**, 1609 (1999).
- [22] B. Z. Kopeliovich, J. Nemchik, A. Schäfer and A. V. Tarasov, Phys. Rev. Lett. **88**, 232303 (2002).
- [23] D. Kharzeev, E. Levin and L. McLerran, Phys. Lett. B **561**, 93 (2003).
- [24] R. Baier, A. Kovner and U. A. Wiedemann, Phys. Rev. D **68**, 054009 (2003).
- [25] J. Jalilian-Marian, Y. Nara and R. Venugopalan, Phys. Lett. B **577**, 54 (2003).
- [26] D. Kharzeev, Y. V. Kovchegov and K. Tuchin, Phys. Rev. D **68**, 094013 (2003).
- [27] J. L. Albacete, N. Armesto, A. Kovner, C. A. Salgado and U. A. Wiedemann, Phys. Rev. Lett. **92**, 082001 (2004).
- [28] A. Accardi and M. Gyulassy, Phys. Lett. B **586**, 244 (2004).
- [29] F. Gelis and R. Venugopalan, Phys. Rev. D **69**, 014019 (2004).
- [30] D. Kharzeev and K. Tuchin, Nucl. Phys. A **735**, 248 (2004).
- [31] K. Tuchin, Phys. Lett. B **593**, 66 (2004).
- [32] J. P. Blaizot, F. Gelis and R. Venugopalan, Nucl. Phys. A **743**, 13 (2004); Nucl. Phys. A **743**, 57 (2004).
- [33] E. Iancu, K. Itakura and D. N. Triantafyllopoulos, Nucl. Phys. A **742**, 182 (2004).
- [34] D. Kharzeev, Y. V. Kovchegov and K. Tuchin, arXiv:hep-ph/0405045.
- [35] L. D. McLerran and R. Venugopalan, Phys. Rev. D **49**, 2233 (1994); J. Jalilian-Marian, A. Kovner, L. D. McLerran and H. Weigert, Phys. Rev. D **55**, 5414 (1997); A. H. Mueller, in *Proceedings of QCD Perspectives on Hot and Dense Matter, Cargese, France, 2001*, edited by J.-P. Blaizot and E. Iancu (Kluwer, Dordrecht, 2002), [arXiv:hep-ph/0111244]; E. Iancu, A. Leonidov and L. McLerran, in *Proceedings of QCD Perspectives on Hot and Dense Matter, Cargese, France, 2001*, edited by J.-P. Blaizot and E. Iancu (Kluwer, Dordrecht, 2002), [arXiv:hep-ph/0202270]; E. Iancu and R. Venugopalan, in *Quark Gluon Plasma 3*, edited by R.C. Hwa and X.N. Wang (World Scientific, Singapore, 2004), [arXiv:hep-ph/0303204].

- [36] N. N. Nikolaev and B. G. Zakharov, *Z. Phys. C* **53**, 331 (1992).
- [37] N. N. Nikolaev and B. G. Zakharov, *J. Exp. Theor. Phys.* **78**, 598 (1994) [*Zh. Eksp. Teor. Fiz.* **105**, 1117 (1994)]; N. N. Nikolaev and B. G. Zakharov, *Z. Phys. C* **64**, 631 (1994).
- [38] B. G. Zakharov, *Yad. Fiz.* **46**, 148 (1987).
- [39] R. J. Glauber, in *Lectures in Theoretical Physics*, edited by W. E. Brittin et al. (Interscience Publishers, Inc., New York, 1959), Vol. 1, p. 315.
- [40] V. N. Gribov, *Sov. Phys. JETP* **29**, 483 (1969) [*Zh. Eksp. Teor. Fiz.* **56**, 892 (1969)].
- [41] N. N. Nikolaev, B. G. Zakharov and V. R. Zoller, *JETP Lett.* **59**, 6 (1994).
- [42] A. H. Mueller and B. Patel, *Nucl. Phys. B* **425**, 471 (1994).
- [43] N. N. Nikolaev and B. G. Zakharov, *Phys. Lett. B* **332**, 184 (1994).
- [44] J. C. Collins and R. K. Ellis, *Nucl. Phys. B* **360**, 3 (1991); S. Catani, M. Ciafaloni and F. Hautmann, *Nucl. Phys. B* **366**, 135 (1991); E. M. Levin, M. G. Ryskin, Y. M. Shabelski and A. G. Shuvaev, *Sov. J. Nucl. Phys.* **54**, 867 (1991) [*Yad. Fiz.* **54**, 1420 (1991)].
- [45] N. N. Nikolaev, W. Schäfer, B. G. Zakharov and V. R. Zoller, *JETP Lett.* **76**, 195 (2002) [*Pisma Zh. Eksp. Teor. Fiz.* **76**, 231 (2002)].
- [46] A. H. Mueller, *Nucl. Phys. B* **335**, 115 (1990).
- [47] N. N. Nikolaev and B. G. Zakharov, *Phys. Lett. B* **332**, 177 (1994).